Water Resources Research

RESEARCH ARTICLE
10.1029/2021WR031149

Identifying Dominant Processes in Time and Space: Time-Varying Spatial Sensitivity Analysis for a Grid-Based Nitrate Model

Songjun Wu[1,2], Doerthe Tetzlaff[1,2,3], Xiaoqiang Yang[1,4], and Chris Soulsby[1,3]

[1]Department of Ecohydrology, Leibniz Institute of Freshwater Ecology and Inland Fisheries, Berlin, Germany, [2]Department of Geography, Humboldt University Berlin, Berlin, Germany, [3]School of Geosciences, Northern Rivers Institute, University of Aberdeen, Aberdeen, UK, [4]Department of Aquatic Ecosystem Analysis and Management, Helmholtz Centre for Environmental Research – UFZ, Magdeburg, Germany

Abstract Distributed models have been increasingly applied at finer spatiotemporal resolution. However, most diagnostic analyses aggregate performance measures in space or time, which might bias subsequent inferences. Accordingly, this study explores an approach for quantifying the parameter sensitivity in a spatiotemporally explicit way. We applied the Morris method to screen key parameters within four different sampling spaces in a grid-based model (mHM-Nitrate) for NO_3-N simulation in a mixed landuse catchment using a 1-year moving window for each grid. The results showed that an overly wide range of aquatic denitrification rates could mask the sensitivity of the other parameters, leading to their spatial patterns only related to the proximity to outlet. With adjusted parameter space, spatial sensitivity patterns were determined by NO_3-N inputs and hydrological transport capacity, while temporal dynamics were regulated by annual wetness conditions. The relative proportion of parameter sensitivity further indicated the shifts in dominant hydrological/NO_3-N processes between wet and dry years. By identifying not only *which* parameter(s) is(are) influential, but *where* and *when* such influences occur, spatial sensitivity analysis can help evaluate current model parameterization. Given the marked sensitivity in agricultural areas, we suggest that the current NO_3-N parameterization scheme (land use-dependent) could be further disentangled in these regions (e.g., into croplands with different rotation strategies) but aggregated in non-agricultural areas; while hydrological parameterization could be resolved into a finer level (from spatially constant to land use-dependent especially in nutrient-rich regions). The spatiotemporal sensitivity pattern also highlights NO_3-N transport within soil layers as a focus for future model development.

Key Points:

- A diagnostic analysis was conducted to disentangle the parameter sensitivity for NO_3-N simulations in catchment modeling in space and time
- Sensitivity differed within sampling spaces, but was controlled spatially by NO_3-N supply/water fluxes while temporally by wetness condition
- Analysis suggests finer-level parameterization needs in arable land, and prioritizes NO_3-N transport in soils for improved conceptualization

Supporting Information:

Supporting Information may be found in the online version of this article.

Correspondence to:

S. Wu,
songjun.wu@igb-berlin.de

Citation:

Wu, S., Tetzlaff, D., Yang, X., & Soulsby, C. (2022). Identifying dominant processes in time and space: Time-varying spatial sensitivity analysis for a grid-based nitrate model. *Water Resources Research*, *58*, e2021WR031149. https://doi.org/10.1029/2021WR031149

Received 2 SEP 2021
Accepted 4 JUL 2022

Author Contributions:

Conceptualization: Songjun Wu, Doerthe Tetzlaff, Xiaoqiang Yang, Chris Soulsby
Methodology: Songjun Wu
Resources: Doerthe Tetzlaff, Chris Soulsby
Supervision: Doerthe Tetzlaff, Chris Soulsby
Writing – original draft: Songjun Wu
Writing – review & editing: Songjun Wu, Doerthe Tetzlaff, Xiaoqiang Yang, Chris Soulsby

1. Introduction

Nitrogen (N) is vital for life (Wetzel, 2001), but its excess is a pollutant that contributes to eutrophication and dead zones in rivers, estuaries, and coastal seas worldwide, with significant economic consequences (Galloway et al., 2008). In Europe, the average N surplus reached 60 kg/ha·yr in agricultural catchments (Leip et al., 2011), which resulted in generally high N levels in rivers (Green et al., 2004), with little improvement despite implementation of EU Water Framework Directive/Nitrate Directive in recent years (Bouraoui & Grizzetti, 2011). Therefore, there remains a need to understand how excess N is transported to river systems, and how it is transformed along dominant flow pathways. However, the underlying hydrological and biogeochemical processes are generally characterized by marked spatiotemporal heterogeneity, with numerous local factors interacting (e.g., climate, topography, soils, and land management practices) (Musolff et al., 2015). As a result of the integrated effect of these numerous processes, which usually have high spatial complexity, the accurate prediction for hydrological and N fluxes is still a challenging task at the catchment scale (Grizzetti et al., 2015).

Spatially distributed modeling is one way to improve predictions of catchment hydrological functioning and nutrient transport processes, as spatial details can be incorporated via regional parameterization (Rozemeijer et al., 2016). More distributed models have been developed and applied over the recent decades, due to the increase in available environmental data and computational resources (Wellen et al., 2015). However, while benefiting from better spatial representation, increased model complexity poses challenges from the increase in parameter numbers, depending on the grid resolution and number of state predictions (Tang et al., 2007). The high-dimensional, nonlinear parameter spaces make it extremely difficult to identify parameter values due to the resulting equifinality (Tonkin & Doherty, 2005), sometimes leading to an intractable and uncertain calibration

due to the exponential increase in computational demands caused by the increasing parameter space dimension (van Griensven et al., 2006). Considering the widespread operational use of distributed models, there remains a need for diagnostic methods capable of better understanding the structure (particularly parameterization) of such models at their full spatial and temporal complexity.

Sensitivity analysis (SA), aiming to quantify how model outputs respond to changes in model inputs, has long been recognized as a helpful diagnostic tool (Saltelli et al., 2004) and widely applied in spatially distributed models (e.g., Berezowski et al., 2015; Hall et al., 2005; Herman et al., 2013a; Lilburne & Tarantola, 2009). However, as shown in Table S1 of Supporting Information S1, most studies have employed the spatial aggregation of input parameters prior to the spatial sensitivity analysis (SSA), which is achieved either by pre-generating the spatial maps/realizations and perturbating the parameters over a certain range (e.g., van Griensven et al., 2006) or directly aggregating the inputs into sub-regions (e.g., Moreau et al., 2013). Such aggregation greatly reduces computational demands, but poses limitations; the sampling space of inputs are generally discrete in the form of spatial maps/realizations (e.g., Anderton et al., 2002), while the spatial heterogeneity of inputs is masked to some extent in the form of sub-regions (e.g., Demirel et al., 2018).

Alternatively, grid-based SSA has the potential to fully incorporate the spatial characteristics of inputs and quantitatively evaluate their impacts on model outputs (e.g., Herman et al., 2013a; Tang et al., 2007; van Werkhoven et al., 2008; Yang et al., 2019). Used as a learning tool, it can help understand and improve model structure (Sieber & Uhlenbrook, 2005), more particularly the parameterization strategy, which is important as the reliability of model predictions largely depends on how well the model is parameterized (Bahremand & De Smedt, 2008; Cornelissen et al., 2016). In general, the existing grid-based distributed models are parameterized based on topography and the physical properties of soils and land cover (Bahremand & De Smedt, 2008). Therefore, SSA at a finer spatial resolution (without spatial aggregation) can either help validate the parametrization if the spatial pattern of parameter sensitivity aligns with the current parameterization scheme (in most case soil/land use-dependent, see Yang et al., 2019), or help unravel the overlooked interactions between parameters and other spatial catchment characteristics (that were not yet included into parameterization) if the spatial sensitivity pattern does not follow the parameterization scheme (Clark et al., 2017). For example, Tang et al. (2007) and van Werkhoven et al. (2008) demonstrated that the spatial distribution of precipitation could also influence the location of identifiable parameter regions, which was usually overlooked in model parameterization. Moreover, the identified spatial domains that are most influential on the model simulations can be targeted for refinement by further data acquisition or higher resolution modeling (Hall et al., 2005).

Parameter sensitivity can also change in time when the actual dominant processes changes due to variation in external forcing (e.g., climate variability, catchment management) (Reusser et al., 2011). Such time-dependent nature of parameter sensitivity has been recognized already ~50 years ago (McCuen, 1973). Consequently, many studies have applied SA in different time periods to explore the temporal dynamics of parameter sensitivity in lumped (Basijokaite & Kelleher, 2021; Ghasemizade et al., 2017; Herman et al., 2013) or distributed models (Guse et al., 2014; Pfannerstill et al., 2015; Reusser et al., 2011). For example, Basijokaite and Kelleher (2021) found that parameter controls on model performance were shaped by a shift in precipitation and air temperature. However, relatively few studies have incorporated analysis of time-variance of parameter sensitivity into a grid-based SSA (Herman et al., 2013a), because it further increases computational demand.

A recently developed water quality model, mHM-Nitrate, provides an opportunity to disentangle parameter sensitivity in both space and time (Yang et al., 2018), as its grid-based structure provides detailed spatial patterns of the processes governing both water and nitrogen fluxes, while the model equations are mostly empirical, constraining the model complexity to an intermediate level (Samaniego et al., 2010). With such adaptations and using of a high-performance cluster, SSA was applied in this study to a 68 km^2 mixed land use catchment (Demnitzer Millcreek catchment, DMC) with intensive agriculture and ~30-year monitoring history in Germany. The sensitivity of key hydrological and NO_3-N parameters was investigated using the Morris method to identify the dominant processes and the most influential locations in the model domain that contribute to model performance. The temporal dynamics of parameter sensitivity have also been explored by applying SSA with a 1-year moving window. Like some SSA studies (Crosetto et al., 2000; Lilburne & Tarantola, 2009), the impacts from the sampling space of parameters were considered, whose importance has been well-documented (Herman et al., 2013b; Sobol, 2001). More specifically, a sequence of four sampling spaces, from crude to well-constrained, was adopted in this study to investigate the impacts of sampling space on parameter sensitivity.

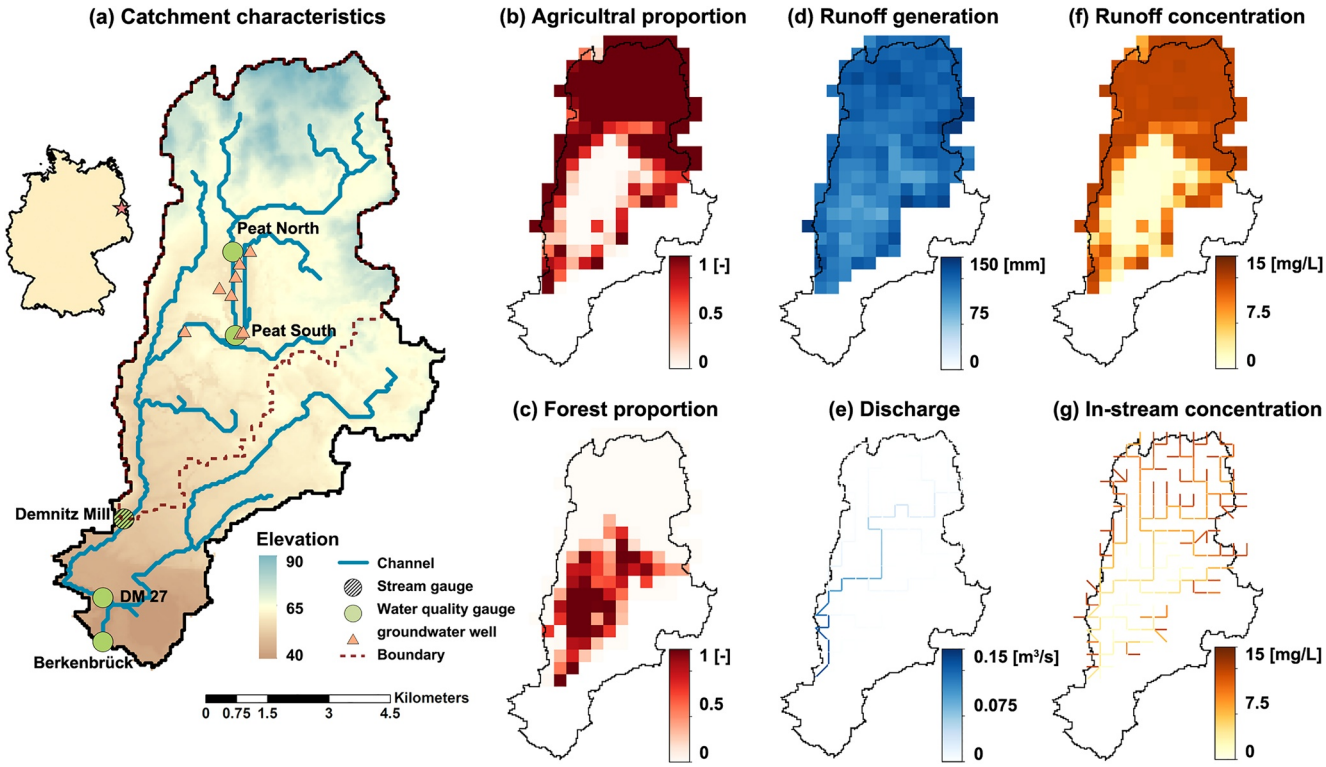

Figure 1. (a) Topography of Demnitzer Millcreek catchment with monitoring locations, (b) proportion of agricultural land use, and (c) forestry cover. The major states and fluxes during 1992–2019 have been simulated in S. Wu et al. (2022), including annual cumulative (d) runoff generation, (e) annual mean discharge, and (f) mean NO_3-N concentration in runoff and (g) discharge.

Through a series of computational experiments, we sought to explore whether and how parameter sensitivities for NO_3-N simulation varied through time and space, and to what extent these were organized by catchment climate and land characteristics. More importantly, we wanted to know how the SSA results could contribute to further model application or development, and how such knowledge can be transferred to other catchments or models. To achieve these goals, the following research questions were addressed:

- What are the spatial and temporal patterns of parameter sensitivity for NO_3-N simulations, and how are they altered by the parameter sampling space?
- Which catchment or climatic characteristics are responsible for these patterns?
- How can the spatiotemporal sensitivity patterns help to evaluate the model parameterization and guide future model development; and to what extent can such knowledge be transferred to other catchments or models?

2. Data and Methods

2.1. Study Catchment

The study site is the 68 km^2 Demnitzer Millcreek catchment (DMC; 52°23′N, 14°15′E), located 55 km SE of Berlin, Germany. The catchment is relatively flat, with an average slope of <2% (Figure 1a). The geology is dominated by ground moraine in the North and glacio-fluvial deposits in the mid-southern sections. The dominant soils are Brown-earths with a high sand proportion (>70%), which leads to a generally high hydraulic conductivity (Kleine et al., 2020). The northern parts are mainly characterized by agricultural land use, including arable land and pasture covering >60% of the catchment area (Figure 1b). Forestry, as the second most dominant land use, increases downstream and accounts for 36% (Figure 1c). There are also several wetlands underlain by peaty soils, with the major one traversed by the main stream (termed as "central wetland" below). Several urban settlements are distributed sporadically in DMC, but the impact on discharge and NO_3-N is limited due to the low population (~5,000 residents) and adequate treatment facilities (Smith et al., 2020).

The catchment experiences a typical mid-continental climate, with relatively low precipitation (~569 mm) and slightly higher potential evapotranspiration (650–700 mm). As a headwater catchment, water balance in DMC is dominated by actual evapotranspiration (>80%) while interflow and groundwater recharge only account for 18% of precipitation (see spatial patterns in Figures 1d and 1e). Prior to 2008, the inter-annual precipitation was characterized by a regular shift (every 1.5–2.5 years) between wet and dry periods, while a tendency toward more clustered wet, then dry periods has been observed since 2008 (S. Wu et al., 2021). This resulted in a prolonged wet (2008–2012) and dry period (since 2013), and a corresponding response of discharge.

In S. Wu et al. (2022), the model mHM-Nitrate was calibrated and validated against in-stream NO_3-N concentrations from five gauges in DMC. Then the long-term NO_3-N balance was estimated as follows: fertilizer application is the main external source of NO_3-N (ranging from 80 to 120 kg/ha·yr in arable), as well as moderate contributions from mineralization (from organic N to NO_3-N, ~30 kg/ha·yr) and wet deposition (~2 mg/L according to the EMEP data for 1995–2005; EMEP, 2001). This results in the spatial distribution and magnitude of NO_3-N dictated by the available NO_3-N sources (Figures 1f and 1g). In contrast, the long-term dynamics of NO_3-N are regulated by the hydrological transport capacity due to the changing hydroclimatic conditions. A negative correlation between in-stream NO_3-N and annual precipitation has been observed (S. Wu et al., 2021).

Land management practices in DMC have gradually changed over the past 30 years. Artificial drainage was historically intensive with deepened and straightened channel network in the northern part of catchment (including arable land and central wetland). These drainage practices ceased in 1990, which led to the gradual re-naturalization of channel characteristics (personal communication with Bösel [2018]). In 2000, more proactive measures were taken to restore the central wetland, including excavating backwaters connected to the main stream, and installing in-channel bunds to reduce channel depth.

2.2. The Morris Method

The Morris method, also known as Elementary Effects (*EE*) method, was used to screen parameter sensitivity. It has long been recognized as a robust diagnostic tool in characterizing significance of inputs on model response (Morris, 1991), which can produce comparable results to variance-based methods (e.g., Sobol, 2001) but with significantly less computation demand (see the comparison of SSA using Morris with $N = 20$ and Sobol's method with $N = 6{,}000$, Herman et al., 2013b). The approach is based on the "one-at-a-time" (OAT) method, which generates a trajectory with a set of starting parameters X, and perturbates each parameter p_i by a variation Δi based on the radial OAT strategy. The elementary effect of ith specific parameter (EE_i) is then obtained:

$$EE_i = \frac{f\left(X_{p_i+\Delta_i}\right) - f\left(X_{p_i}\right)}{\Delta_i} \tag{1}$$

where f denotes the evaluation metrics used for sensitivity analysis. In this study, the root mean squared error (RMSE) and percent bias (PBias) were used (see Equations 4 and 5 in Section 2.5).

The *EE* calculation needs to be iterated multiple times, as a single *EE* depends strongly on the location of the initial point X in the parameter space. Therefore, multiple (r) trajectories with different initial point X and the perturbation Δ_i were sampled to compute two sensitivity indices, mean (μ^*) and standard deviation (σ) of the absolute value of elementary effects across the r trajectories (Campolongo et al., 2007), which represent the global sensitivity of each parameter and its interaction with other parameters, respectively.

$$\mu_i^* = \frac{\sum_{j=1}^{r} |EE_i^j|}{r} \tag{2}$$

$$\sigma_i = \sqrt{\frac{1}{r-1}\sum_{j=1}^{r}\left(|EE_i^j| - \mu_i^*\right)^2} \tag{3}$$

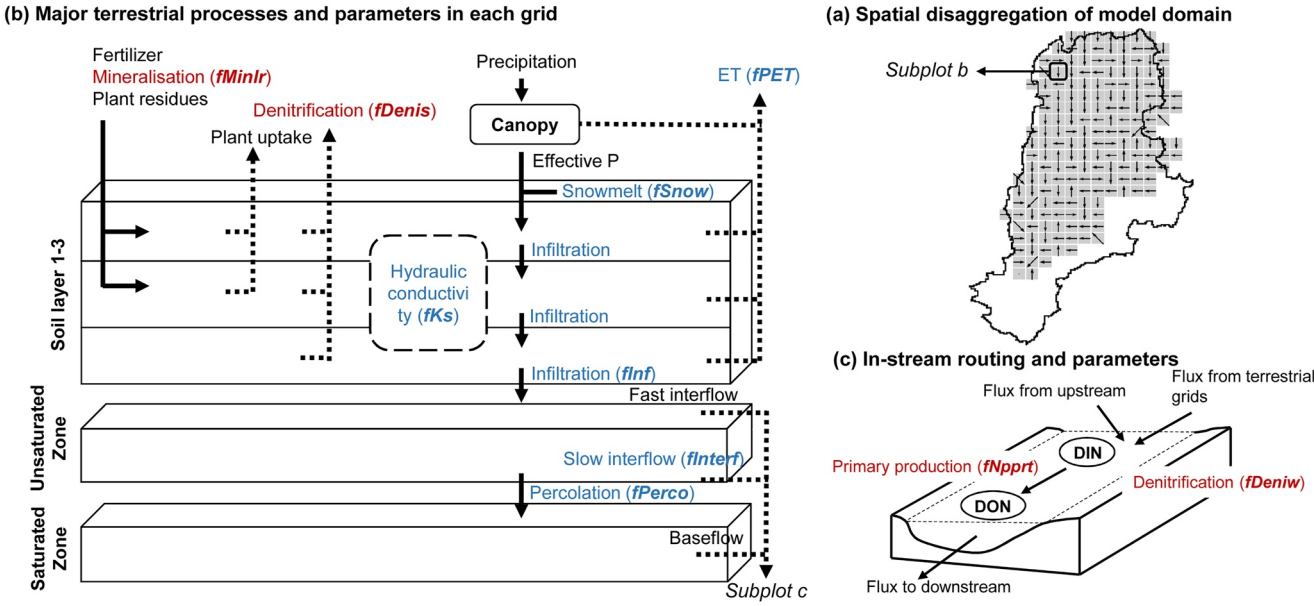

Figure 2. (a) The spatial disaggregation strategy, (b) processes and structure of each terrestrial grid, and (c) in-stream routing and processes. The hydrological and NO_3-N parameters selected for spatial sensitivity analysis in this study were marked as blue and red, respectively.

2.3. The Model mHM-Nitrate

2.3.1. Model Structure and Parameterization

The water quality model mHM-nitrate was recently developed (Yang et al., 2018) by integrating a nitrogen sub-model into the fully distributed hydrological platform (mHM; Samaniego et al., 2010). The model's robust capacity to simulate hydrological and NO_3-N fluxes in mesoscale catchments has been verified in several applications (S. Wu et al., 2022; Yang et al., 2019). A conceptual diagram of the model structure is presented in Figure 2. For detailed descriptions of model formulas please refer to Yang et al. (2018), as only a brief introduction on the key components and dominant processes follows.

The hydrological sub-model was fully adopted from the mHM model (Samaniego et al., 2010), with hydrological processes including canopy interception (Dickinson, 1984), snow accumulation and melt (Hundecha & Bárdossy, 2004), evapotranspiration from canopy and soils, infiltration between soil layers, percolation into deeper aquifer, and runoff generation (Bergström, 1995). The runoff is composed of three components: faster interflow, slow interflow, and baseflow, which represent the overland flow, shallow subsurface flow, and deep groundwater flow, respectively. All these processes are simulated independently in each grid, then the generated runoff is routed to downstream grid(s) using the Muskingum flood routing algorithm (Gill, 1978). The parameterization was adopted from mHM (details in Samaniego et al. [2010]), where most parameters were identical over the model domain, with several parameters in snow, soil moisture, and interflow modules being land-use dependent. The baseflow generation was related to the geology types.

In the nitrogen sub-model, nitrogen is categorized into organic (DON) and inorganic (DIN) forms, the latter of which is treated as equivalent to NO_3-N in this study, as ammonium and nitrite respectively account for less than 15% and 1% of fluxes in natural environments (Meybeck, 1982). The transport of nitrogen follows the hydrological pathways; both ON and IN are assumed to be fully mixed in each reservoir in each timestep.

The transformation of nitrogen is mainly modified from Hydrological Predictions for the Environment (HYPE), a well-tested water quality model (Lindström et al., 2010). The terrestrial processes describe the transformation between four different forms: active and inactive soil organic nitrogen (SON_A, SON_i), and dissolved organic and inorganic nitrogen (DON, DIN). These processes include soil denitrification (from DIN to gaseous nitrogen leaving the system), mineralization (from DON/SON_A to DIN), dissolution (exchanges between SON_A and DON) and degradation (from SON_I to SON_A). In-stream processes consist of aquatic denitrification (DIN reduction in the channel network) and assimilation (from DIN to DON). The rate of each transformation process is the function of

Table 1
The Parameters Selected for Spatial Sensitivity Analysis With Descriptions and Default Parameterization Strategy in mHM-Nitrate

Parameter	Description	Parameterization	PS1		PS2		PS3		PS4	
			Min	Max	Min	Max	Min	Max	Min	Max
fsnow	Temperature threshold for snow accumulation/melt	General	−2	2	−2	2	−2	2	−2	2
fKs	Reference hydraulic conductivity	General	6e−3	2.6e−2	6e−3	**1.2e−2**	6e−3	2.6e−2	6e−3	**1.2e−2**
fPET	Minimum coefficient for aspect correction of PET	General	0.7	1.3	0.7	**0.9**	0.7	1.3	0.7	**0.9**
fInf	Correlation of shape factor of soil infiltration	General	1	4	1	4	1	4	1	4
fInterf	Recession factor of slow interflow generation	General	1	30	1	**12**	1	30	1	**12**
fPerco	Recharge coefficient of percolation	General	0	50	**10**	50	0	50	**10**	50
fDeniw	Reference denitrification rate in stream water	Land use	1e−8	5.0e−2	1e−8	5.0e−2	1e−8	**6.6e−3**	1e−8	**6.6e−3**
fDenis	Reference denitrification rate in soils	Land use	1e−8	1.1	1e−8	1.1	1e−8	**1.0e−2**	1e−8	**1.0e−2**
fNpprt	Reference primary production rate in stream water	Land use	1e−8	1	1e−8	1	1e−8	**1.8e−2**	1e−8	**1.8e−2**
fMinlr	Reference mineralization rate in water and soils	Land use	1e−4	8e−1	1e−4	8e−1	1e−4	8e−1	1e−4	8e−1

Note. The PS1-4 respectively represents the parameter set with no constraint (PS1), hydrological parameters constrained (PS2), NO_3-N parameters constrained (PS3), and both parameters constrained (PS4). The changed values are shown in **boldface**.

a reference rate corrected by several factors including temperature, soil moisture, soil nitrogen storage, etc. The reference rate is pre-setup for each land use type according to the parameters in nitrogen sub-model. In the other words, the transformation rate is a linear function of the corresponding NO_3-N parameters, whose parameterization is land use dependent.

2.3.2. Data Acquisition and Model Setup

The meteorological data required for mHM-Nitrate include daily precipitation, air temperature, and potential evapotranspiration (PET). The first two variables were acquired and interpolated from three weather stations maintained by the German Weather Service (DWD), while potential evapotranspiration, as the reference evapotranspiration in mHM-Nitrate, was estimated using the Penman-Monteith method. Daily discharge has been monitored at two gauges, Demnitz Mill and Berkenbrück since 1992. In-stream NO_3-N was monitored by weekly grab sampling at the two discharge gauges and three additional sites (Peat North, Peat South and DM27, Figure 1a). DEM, soil, land use, and geology maps were resampled into 50 m resolution for model initialization and parameterization, while daily simulation of discharge and NO_3-N was setup using 500 m^2 grid size for both terrestrial and in-stream phase, which resulted in a total of 185 grids. The simulation covered the relatively long period since 1992, with the antecedent two years as warming period.

2.4. Preparatory Procedures for Time-Varying SSA

2.4.1. Identifying the Parameters for Time-Varying SSA

Given the large parameter number in mHM-Nitrate (>80), it is not feasible to include all parameters into time-varying SSA due to its expensive computational cost. In the other words, it is necessary to first exclude the insensitive parameters to mitigate the computational demands for further time-varying SSA. Therefore, a prior sensitivity analysis was conducted based on the default parameterization strategy, that is, the parameters were either consistent over the model domain or assigned based on land use types, soil types and geology types (see Section 2.2). The Morris method was employed to rank the parameter sensitivity according to their influence on RMSE between simulated and observed in-stream NO_3-N at Demnitz Mill during 1992–2019 (Figure S1 in Supporting Information S1). The default parameter space in mHM-Nitrate was used. Accordingly, the most sensitive parameters were identified (*fSnow*, *fKs*, *fPET*, *fInf*, *fInterf*, *fPerco*, *fDeniw*, *fDenis*, *fNpprt*, *fMinlr*), which respectively corresponded to the key hydrological (snow accumulation and melt, soil moisture dynamics, infiltration, interflow, and groundwater flow generation) and NO_3-N processes (aquatic and soil denitrification, aquatic assimilation, and soil mineralization). Then these 10 parameters were further transferred into time-varying SSA (see Section 2.5). For parameter description please refer to Table 1.

2.4.2. Model Calibration

Another barrier for SSA is the quality of observed data, as some gaps exist in discharge and NO_3-N time series due to the funding limitation, though they have been monitored at multiple sites since 1992 in DMC. These data gaps can significantly bias the sensitivity ranking when a small window length was adopted for SSA (e.g., 1 year in this study). Therefore, reconstructing the time series to fill the data gaps was necessary, and a model calibration was conducted to achieve this goal.

In brief, mHM-Nitrate was calibrated by 50,000 iterations using the Dynamically Dimensioned Search method (Tolson & Shoemaker, 2007). The model performance was successfully validated at multiple monitoring sites, confirming the spatial representation of optimized parameter set. As the calibration is not the focus of this study, a summary of the method and performance of calibrated parameters are given in Text S1, Table S2, and Figure S2 of Supporting Information S1. For full details please refer to S. Wu et al. (2022).

With the calibrated model, the simulated time series of in-stream NO_3-N (Figure S2 in Supporting Information S1) were used as reference model run for time-varying SSA, while the other states and fluxes (Figure S3 in Supporting Information S1) were used for post-analysis of the SSA results (i.e., identifying the potential cause of spatiotemporal sensitivity patterns by examining the relationship between SSA results and the simulated internal states and fluxes).

2.5. Computation Design for Time-Varying SSA

In order to investigate the spatiotemporal characteristics of parameter sensitivity, three sequential experiments were conducted. First of all, four sampling spaces of parameters were selected for the key hydrological and NO_3-N parameters (Table 1) in Experiment A, to explore the impact of parameter sampling space. Second, SSA was applied in the four selected parameter spaces over the whole period (1992–2019) in Experiment B, which aimed to unravel the spatial patterns of parameter sensitivity against the simulated NO_3-N time series at Demnitz Mill. In Experiment C, the temporal dynamics of the spatial sensitivity patterns over the past 30 years were explored using time-varying SSA based on a 1-year moving window. The correlation between sensitivity indices and catchment characteristics were examined using Spearman and Pearson tests.

2.5.1. Experiment A: Identifying the Ranges for Hydrological and NO_3-N Parameters

Four typical sets of parameter space (termed as PS1-4; Table 1) were selected for the following SSA, which respectively represent the default parameter space in mHM-Nitrate, and parameter space with hydrological parameters constrained, NO_3-N parameters constrained, and both parameters constrained.

The ranges of the original parameter set (PS1) were derived from the default setting of mHM-Nitrate, which has been successfully tested in different catchments (S. Wu et al., 2022; Yang et al., 2018).

Due to the high non-linearity and empirical equations in the hydrological simulation, an experience-based constraint on hydrological parameter space is impossible. Instead, the constraints on hydrological parameters were determined by evaluating model performance (NSE) over the full range of PS1 values. More specifically, 10,000 parameter sets were sampled from the original parameter space PS1 of mHM-Nitrate using the Latin-Hypercube (LH) method (Helton & Davis, 2003). The resulting NSEs for discharge at Demnitz Mill were plotted against the parameter values (Figures 3a and 3b) and NSEs for in-stream NO_3-N (Figure S4 in Supporting Information S1). Also, the relationship between parameter values and model performance was checked in the form of logarithmic discharge (Figure S5 in Supporting Information S1). Accordingly, the hydrological parameters were constrained based on the posterior parameter space leading to a better fit between the simulated and observed discharge (NSE > 0.5), and termed as PS2 (Table 1).

Differing from the hydrological parameters, all NO_3-N parameters were regarded as the reference rates and linearly correlated to the corresponding processes in mHM-Nitrate; therefore, the rough bounds of NO_3-N parameter could be obtained from the experience in previous field surveys and modeling calibrations (S. Wu et al., 2022). More specifically, the maximum caps of NO_3-N parameters were set up as double of the previously calibrated rates in DMC (S. Wu et al., 2022), which in general span the possible parameter space in practice according to the calibration experience. The constrained bounds were termed as PS3.

Ultimately, both hydrological and NO_3-N parameters were constrained and termed as PS4 (Table 1).

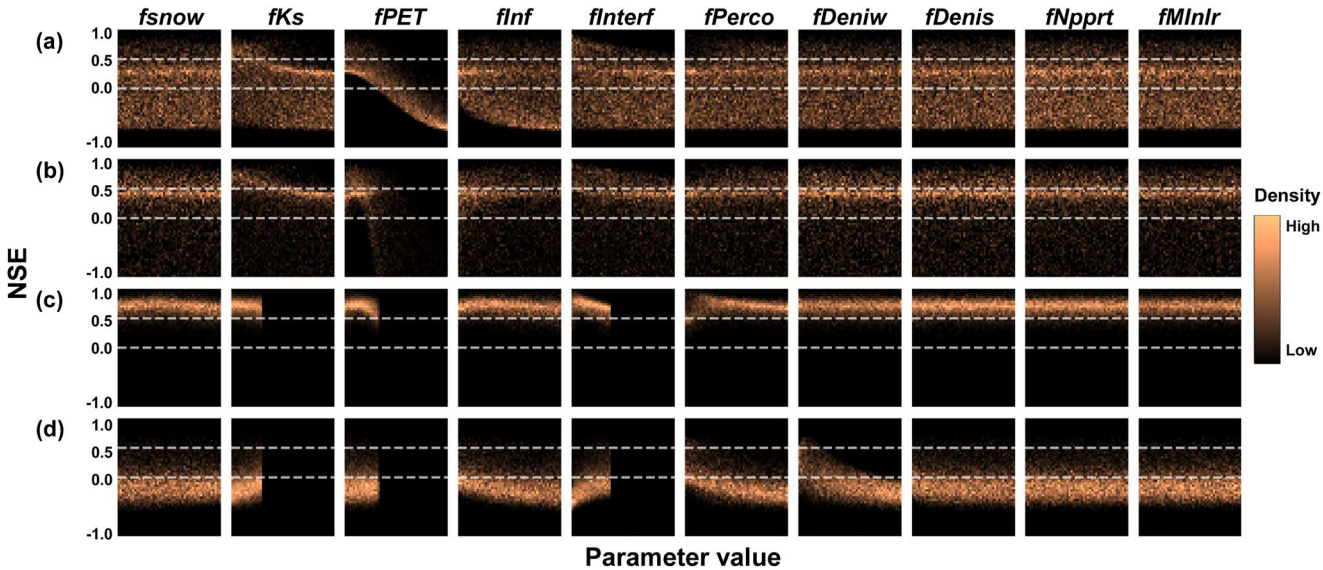

Figure 3. The distribution of model performance (NSE between simulation and observation) against parameter values, including the (a) discharge and (b) NO_3-N performances against 10,000 PS1 parameters, and the (c) discharge and (d) NO_3-N performances against 10,000 PS2 parameters. The two lines respectively denote NSE = 0.5 and NSE = 0.

2.5.2. Experiment B: SSA Application Against NO_3-N at Demnitz Mill

SSA was applied for the 10 influential parameters selected in Section 2.4 (Table 1) with the Morris method across the four parameter space from Experiment A. The major difference from SA is that a full spatial disaggregation strategy was employed for the model parameterization for SSA: in normal SA, parameters were either spatially constant or land use/soil type-dependent, while in SSA, parameters were separately assigned in each grid. In the other words, for each model run, rather than simply assigning a value for the whole model domain (for global parameters) or for each land use/soil type (land use/soil-dependent parameters) in normal SA, a spatial map is needed to parameterize each of the 10 parameters in SSA. This resulted in a total of 185 grids × 10 parameters = 1,850 parameters. The LH sampling method was selected for trajectory generation in the Morris method (i.e., the initial/starting point X of each parameter and the perturbation Δ_i, see Equation 1) for a better representativeness of the feasible parameter space (Helton & Davis, 2003). To ensure the robustness of the sensitivity results, we used a relatively large number of trajectories (r = 80; see the confidence interval plots in Figure S6 of Supporting Information S1), which resulted in the total number of model evaluations reaching $(1{,}850 + 1) \times 80 \times 4 = 592{,}320$.

Similar to other SSA studies (e.g., Herman et al., 2013a), the sensitivity indices of parameters were calculated based on the model performance metrics rather than the output time series. The model was run for the period 1992–2019 (with a 720-day warm up period); then RMSE and PBias, which respectively focus on the simulation of peak values and long-term balance, between the simulated and observed in-stream NO_3-N at Demnitz Mill were computed:

$$\mathrm{RMSE} = \sqrt{\frac{1}{n}\sum_{i=1}^{n}\left(N_{S,i} - N_{O,i}\right)^2} \tag{4}$$

$$\mathrm{PBias} = \frac{\sum_{i=1}^{n} N_{S,i} - \sum_{i=1}^{n} N_{O,i}}{\sum_{i=1}^{n} N_{O,i}} \tag{5}$$

where n denotes the total timesteps of the simulation period (9863 in this experiment); $N_{S,i}$ and $N_{O,i}$ represent the simulated and observed NO_3-N at ith timestep at Demnitz Mill (the catchment outlet). These two metrics were then used for sensitivity ranking.

To avoid the disturbance of data gaps or uneven distribution of data points, the simulated in-stream NO_3-N at Demnitz Mill from a prior calibration (see Section 2.4 and Figure S2 in Supporting Information S1) was used as

reference model run for SSA in this study. Such virtual datasets have been commonly used in modeling studies, such as Berezowski et al. (2015), Hostache et al. (2010), and van Werkhoven et al. (2008).

2.5.3. Experiment C: Time-Varying SSA Against NO_3-N at Demnitz Mill

The time-varying SSA shared the same model evaluations and simulated results for the SSA over the whole period in Experiment B. The difference was that the sensitivity indices were no longer computed only once for the entire period 1992–2019, but using a 1-year moving window with a 2-month time step. Accordingly, the sensitivity indices μ^* of 1,850 parameters (also derived from RMSE and PBias) were calculated at a total of 313 intervals over the past 30 years.

Besides μ^*, the relative sensitivity of parameters ($R\mu^*$) was calculated to explore the dominant parameter(s) during a specific period. More specifically, the relative sensitivity of ith parameter ($R\ \mu^*_{i,t}$) was calculated via dividing its $\mu^*_{i,t}$ by the summed μ^* of 1,850 parameters ($\sum_{j=1}^{1850} \mu^*_{i,t}$) in the tth moving window:

$$R\mu^*_{i,t} = \frac{\mu^*_{i,t}}{\sum_{j=1}^{1850} \mu^*_{i,t}} \tag{6}$$

where j denotes the number of all parameters in tth moving window. The calculation was repeated in each moving window, and the temporal dynamics were investigated by calculating the Spearman correlation coefficient between the time series of precipitation and $R\mu^*$ for each parameter in each grid (Figure S15 in Supporting Information S1).

Apart from this, $R\mu^*$ was aggregated over the model domain:

$$\text{Aggregated } R\mu^*_{k,t} = \frac{\sum_{s=1}^{185} R\mu^*_{k,s,t}}{185} \tag{7}$$

where k denotes the aggregated parameter (10 in total, see Table 1), $R\mu^*_{k,s,t}$ represents the relative sensitivity of the parameter k in sth grid in tth timestep. The temporal trends of relative sensitivity were also investigated by calculating the Spearman (Figure 7) and Pearson (Figure S16 in Supporting Information S1) correlation coefficients between aggregated $R\mu^*_{k,t}$ and hydrological and NO_3-N states/fluxes (Figure S3 in Supporting Information S1).

3. Results

3.1. Parameter Space and Model Performance (Experiment A)

The model performance was first analyzed in the default parameter space of the mHM-Nitrate. As shown in Figure 3a and Figure S5a in Supporting Information S1, most hydrological parameters had an effective space which resulted in a better simulation of discharge. Accordingly, the ranges of *fKS*, *fPET*, *fIntef*, *fPerco* were constrained while *fSnow* and *fInf* remained unchanged (PS2 in Table 1). To verify the constrained parameter space, an additional validation was conducted by sampling 10,000 parameter sets from the new parameter space and evaluating their performance. The new hydrological parameter space seemed robust with NSEs of most simulations >0.5 (Figure 3c).

In contrast, no specific space for NO_3-N parameters could be identified for an improved model performance (Figure 3b). Moreover, the hydrological and NO_3-N simulations were disconnected, as the correlation between the discharge and NO_3-N simulation was not positive. According to Figures 3a and 3b, the hydrological parameter space which resulted in better hydrological simulations was different from the one leading to better NO_3-N simulations. Besides, the NO_3-N simulations were still unsatisfactory in Figures 3c and 3d, though the discharge simulations were good (NSE > 0.5). Further evidence for the disconnection of hydrological and NO_3-N simulations can be found when we screened the hydrological and corresponding NO_3-N performance in the 10,000 iterations (in Figure S4a of Supporting Information S1): the correlation became negative when NSE of discharge >0.5. This

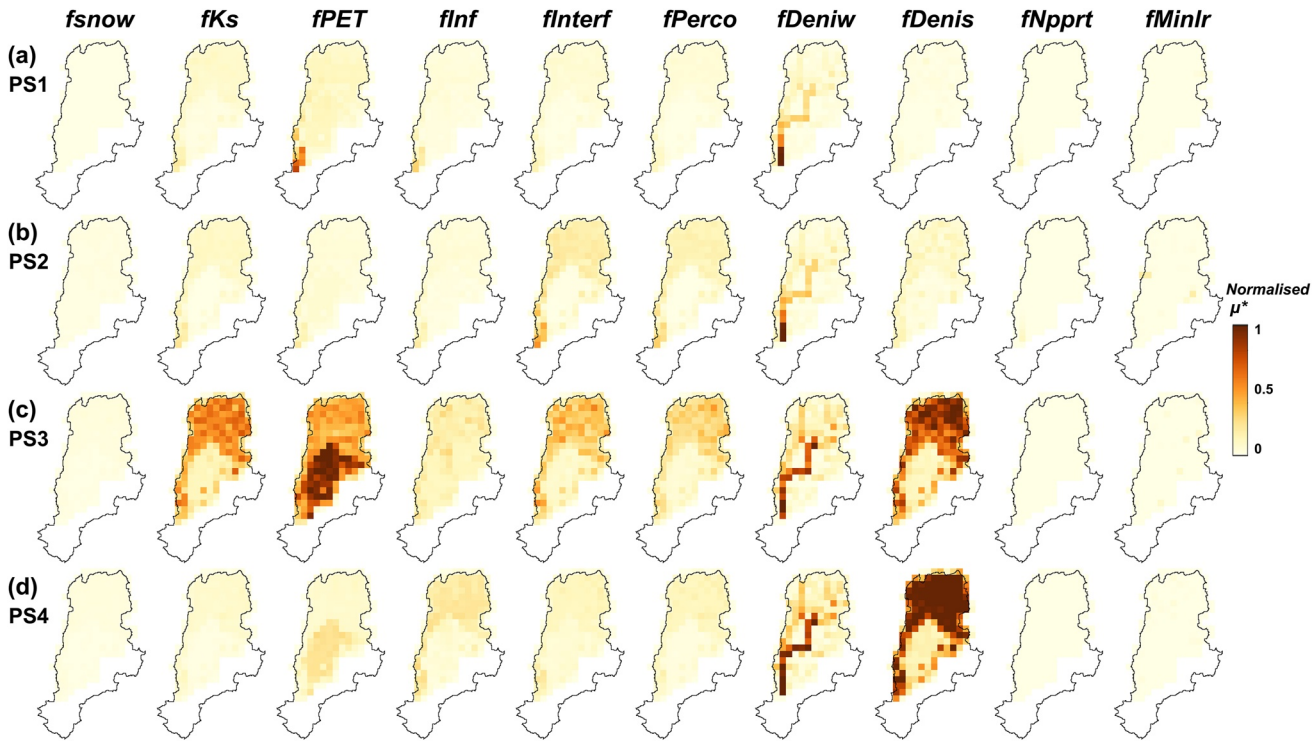

Figure 4. The spatial distribution of parameter sensitivity (μ^*) based on root mean squared error of NO_3-N at the outlet. Four sets of parameters (PS1-4, Table 1) were tested and μ^* values were shown in panels (a–d) accordingly. All subplots share the same color code, in which μ^* ranges within [0–0.01].

means the increase in discharge simulations resulted in a deterioration in NO_3-N simulations, indicating that a realistic hydrological simulation is not a prerequisite of a good NO_3-N simulation.

3.2. Spatial Distribution of Parameter Sensitivity (Experiment B)

RMSE and PBias metrics produced similar spatial and temporal patterns of parameter sensitivity, so only RMSE-based results are presented in the main text, while PBias-based results are shown in the Supporting Information.

Spatial patterns of parameter sensitivity were distinct in the different sampling spaces (Figure 4). In PS1 and 2, NO_3-N simulation was generally dominated by the aquatic denitrification in grids with channel, while the rest of the parameters only showed limited influence on model performance. This pattern is also clear when the dominant parameter was screened over the model domain (Figure S13 in Supporting Information S1). More specifically, only *fPET* showed slight impacts in PS1 while the sensitivity of almost all hydrological parameters in PS2 was damped. In contrast, most parameters were activated when NO_3-N parameters were effectively constrained in PS3 and 4. *fPET*, *fKS*, and *fDenis* all became remarkably influential in the constrained parameter space; the process-controls on runoff generation (*fInterf* and *fPerco*) also exerted moderate impact on model performance. Moreover, the constraint on NO_3-N parameters significantly changed the spatial patterns of parameter sensitivity. In PS1 and 2, the parameter sensitivity in the terrestrial phase largely depended on the proximity of the outlet, that is, a higher sensitivity when being closer to the outlet. This was especially clear for the hydrological parameters, for example, *fKs*, *fPET*, and *fInf* in PS1, and *fInterf* and *fPerco* in PS2, which merely showed sensitivity in the domain near the outlet.

In contrast, with a constrained sampling space for NO_3-N parameters, the location of grids only showed a minor impact on several parameters (*fInf*, *fInter*, and *fPerco*) in PS4, while parameter sensitivity in PS3 was almost independent from the outlet proximity. Catchment characteristics, instead, became the dominant factor, as the sensitivity of almost all hydrological parameters exhibited a strong positive correlation with the proportion of arable land. Besides, the hydrological fluxes in DMC were also land-use-dependent, being lower in agricultural

areas due to the lack of canopy interception and evapotranspiration (Figures 1d and 1e), which implied that better hydrological transport capacity and greater runoff fluxes contributed to the higher parameter sensitivity. The only exception was *fPET*, which showed an opposite pattern with higher sensitivity in forested area. As for NO_3-N parameters, the sensitivity of *fDenis* also followed the distribution of agricultural land use, while *fDeniw* mainly increased along the main stream.

The constraint on hydrological parameter space also moderately altered parameter sensitivity. Damped sensitivity of *fKs* and *fPET* was the direct result of smaller parameter spaces (from PS1 to PS2, and from PS3 to PS4). Instead, the sensitivity of *fInterf* and *fPerco* increased in PS2 while *fInf* increased in PS3. It is clear that better-constrained hydrological simulation resulted in a sensitivity shift from the initial soil moisture storage (in upper soil columns) to the subsequent infiltration or runoff generation processes (in lower columns and underlying aquifers). In terms of NO_3-N parameters, the soil denitrification process was more influential (*fDenis*) when hydrological parameter space was effectively constrained.

Though parameter space greatly changed the spatial distribution of parameters sensitivity, the impact of *fSnow*, *fNpprt*, and *fMinlr* on model performance was negligible at all times, regardless of the change in sampling space.

As for sensitivity indices σ, which represents the interaction between parameters, generally followed the spatial pattern of μ^*. A moderate difference can be found in *fDeniw*, as high σ values were only observed near the outlet or along the main stream (Figures S9 and S11 in Supporting Information S1) while μ^* clearly expanded to upstream area (Figure 4 and Figure S7 in Supporting Information S1). Similar to the parameter sensitivity, different evaluation metrics only led to limited discrepancy (see RMSE in Figure S9 of Supporting Information S1 and PBias in Figure S11 of Supporting Information S1).

3.3. The Temporal Variability of Parameter Sensitivity (Experiment C)

Figure 5 shows the temporal dynamics of RMSE-based parameter sensitivity μ^*, which was generally positively correlated to wetness conditions regardless of sampling space. This was most evident in 2008–2010, when a prolonged wet period persisted and all the parameters (PS1-4) exhibited a stronger influence on model performance. In contrast, the sensitivity was more damped after 2012, when a ~7-year dry period started. The temporal dynamics of sensitivity indices σ (Figures S10 and S12 in Supporting Information S1) also aligned with the indices μ^*, thus the following text mainly focused on the temporal pattern of μ^*.

Interestingly, a general increased sensitivity μ^* of denitrification in both stream water and soils were found after 2000, when the wetland restoration took place. The average sensitivity indices of *fDeniw* and *fDenis* in the whole model domain were respectively 10/57% and 54/55% lower for PS3/4 before 2000 than the average afterward (Figures 5c and 5d). This discrepancy was somewhat independent from the hydro-climatic conditions; for example, the sensitivities of *fDeniw* and *fDenis* in 1994 were 61/43% and 75/62% lower than those in 2010, despite the annual precipitation being similar (709 and 707 mm in 1994 and 2010, respectively).

Differing from the uniformly positive response of parameter sensitivity to annual wetness conditions, the relative proportion of parameter sensitivity ($R\mu^*$, here termed as relative sensitivity, see Section 2.5) provided more information on the long-term shift in the dominant processes. First, we checked the correlation between annual precipitation and relative sensitivity for each parameter in each grid. The results (Figure S15 in Supporting Information S1) showed that at grid level the sensitivity indices $R\mu^*$ was either positively or negatively correlated to precipitation for most parameters, and such correlation remained consistent over the catchment domain. There were several exceptions including *fKs*, *fInterf*, and *fPerco*, exhibiting a moderately contrasting correlation between forested and non-forested areas, but there was no co-existence of highly positive and negative correlation for the same parameter ($|Corr| > 0.5$). In the other words, the relative sensitivity $R\mu^*$ shared a similar temporal trend over the model domain for most parameters. Such consistent spatial distribution of temporal sensitivity dynamics provided a robust evidence base for the next step, aggregating the relative sensitivity over the model domain (Figure 6).

In general, the temporal trends of cumulative relative sensitivity of six hydrological parameters were complex (Figure 6a) and the shift in parameter dominance was observed during the transition between wet and dry years (see the most dominant parameter over space and time summarized in Figure S14 of Supporting Information S1). Similar to the spatial patterns, the aggregated relative sensitivity of parameters was greatly altered by

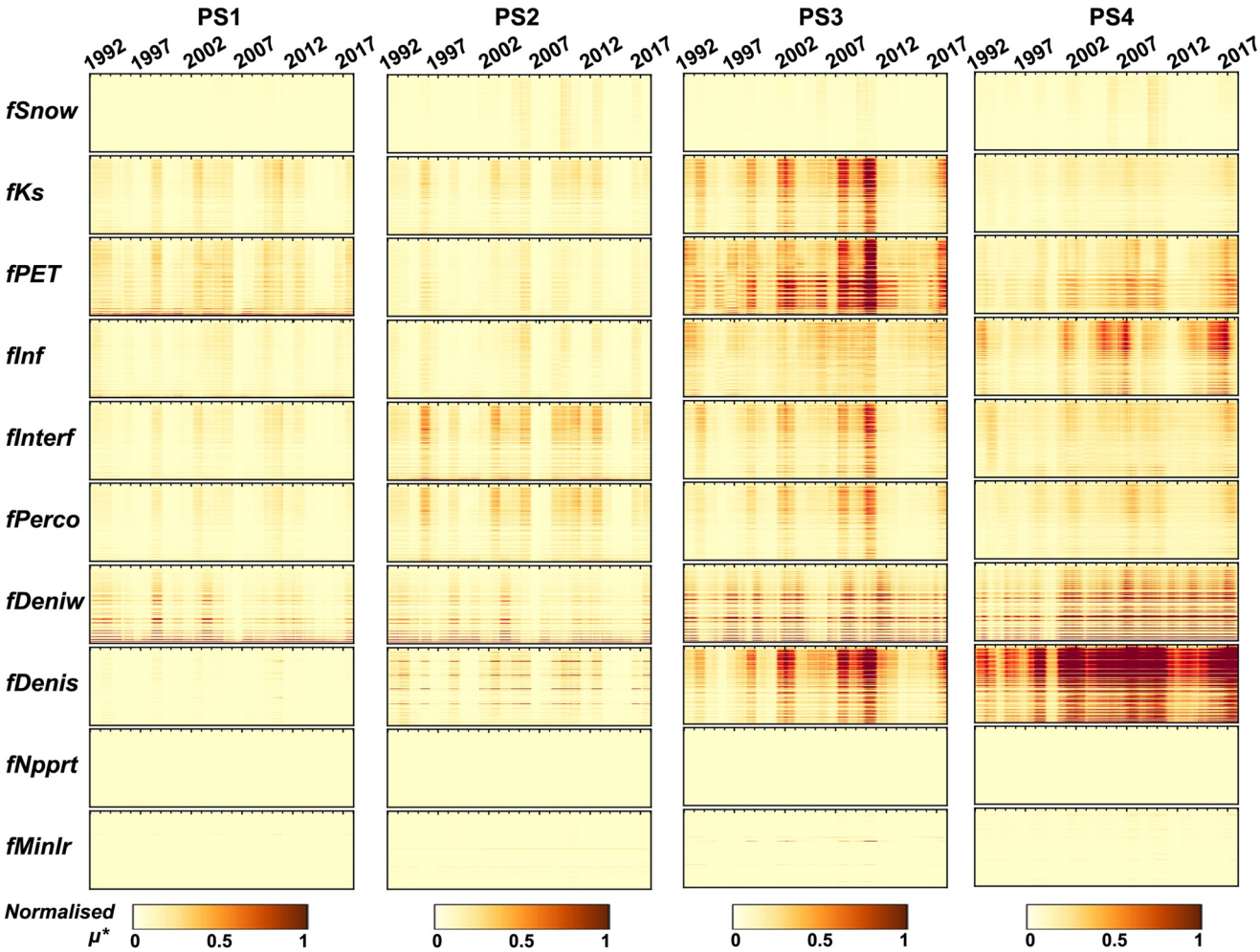

Figure 5. Time-varying sensitivity indices μ^* based on root mean squared error of NO_3-N at the outlet. The *y*-axis shows the 185 grids arranged from upstream to downstream.

the sampling space (Figure 6); and their correlation with catchment characteristics could be opposite in different sampling space (Figure 7). For example, the cumulative hydrological sensitivity in PS3 was positively related to the annual precipitation, while a negative correlation was observed in PS2 and 4. Such contrasting correlations in different sampling space were also found in the snow-melt threshold *fsnow*. In contrast, consistent temporal patterns of relative sensitivity were found in the remaining parameters, regardless of the varied sampling space. The reference hydraulic conductivity (*fKs*) and parameters related to runoff generation (*fInterf* and *fPerco*) were more influential on model performance in wetter years, while *fPET* and *fInf* exhibited an opposite pattern: strong negative correlation with annual precipitation and all hydrological fluxes. Such opposing influence of different parameters somewhat explained the difficulty in summarizing the temporal trend of cumulative hydrological sensitivity.

Unlike the complexity in hydrological parameters, the temporal trends of NO_3-N parameters generally stayed consistent in different sampling spaces (Figure 7). Their correlations with hydrological fluxes were determined by whether the corresponding process was in the terrestrial or in-stream phase. The relative sensitivity of parameters in soil layers (*fDenis* and *fMinlr*) exhibited a negative correlation with hydrological fluxes, which means greater influence of soil denitrification and mineralization on NO_3-N simulation in wetter years. In contrast, the in-stream parameters (*fDeniw* and *fNpprt*) exerted stronger impacts in drier years, resulting in a negative correlation with the hydrological fluxes.

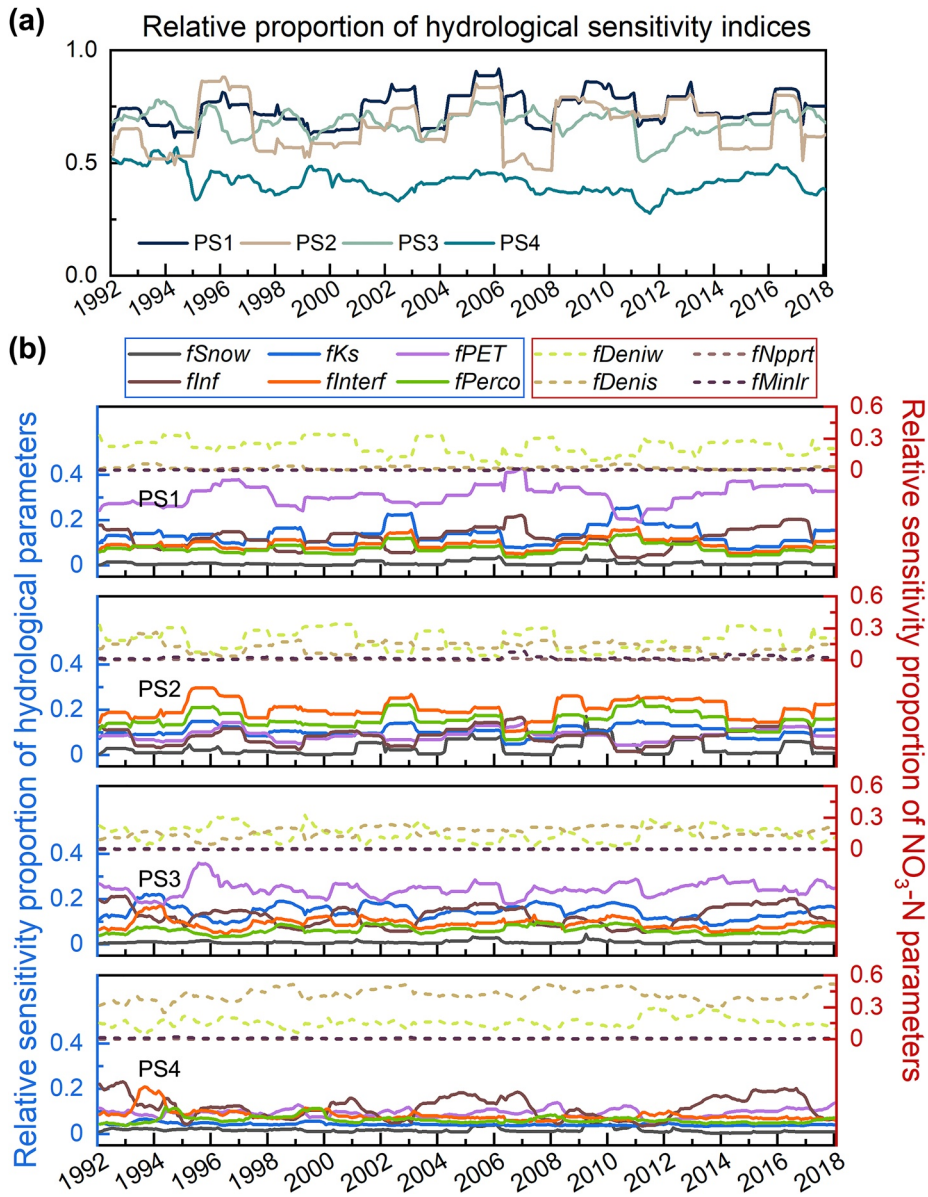

Figure 6. (a) The relative proportion of parameter sensitivity since 1992. The cumulative sensitivity of all hydrological parameters and (b) the sensitivity of individual hydrological and NO_3-N parameters are shown.

4. Discussion

Sensitivity analysis (SA) has been widely applied as a diagnostic tool to quantify how model outputs respond to changes in model inputs and to evaluate the model structure (Saltelli et al., 2004; Sarrazin et al., 2016). However, its implementation in spatially explicit context (grid-based) have been limited due to the expensive computation demands (Herman et al., 2013a). This is particularly the case for water quality modeling, because relatively few grid-based SSA have been applied in simulations of NO_3-N and other important pollutants (e.g., Yang et al., 2019). As Koch et al. (2017) stated, a formal approach of how to assess the global sensitivity of spatially distributed input parameters is still lacking. With the goal to further complement both the methodology and interpretation of SSA, we evaluate the SSA application regarding the selection of parameter space (in Section 4.1), and summarize the spatiotemporal pattern of parameter sensitivity and the potential causes (in Section 4.2 and 4.3). Moreover, the wider implications from this analysis, that is, how SSA results help to evaluate the parameterization scheme, identify the influential process for future development and guide the refinement of observation

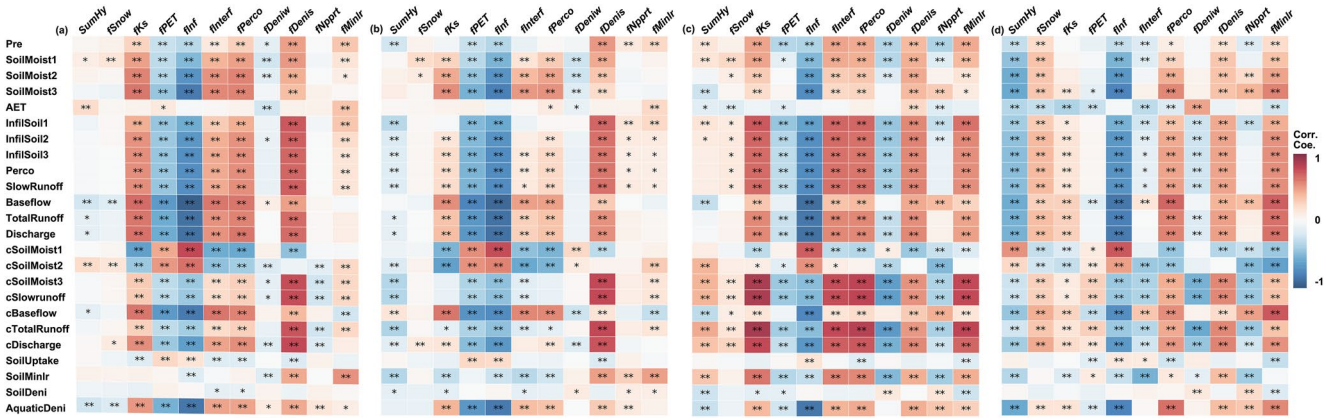

Figure 7. (a–d) The Spearman correlation coefficients between the parameter sensitivity (root mean squared error-based) and catchment characteristics in PS1-4. Significance and high significance were considered when $p < 0.05$ and 0.01, and were marked as "*" and "**" respectively. For abbreviations of catchment characteristics please refer to Table A1.

networks are discussed (in Section 4.4). The transferability to other catchments or models and the corresponding uncertainty are also briefly introduced.

4.1. Influence of the Selection of Parameter Space

Parameter sampling space is fundamental in SA, which can greatly affect or even dominate the results (Saltelli et al., 2004). In this study, four sets of parameters (from crude to well-constrained) were employed, resulting in distinct patterns of parameter sensitivity, and thus underlined the importance of the sampling space for the SSA results. Though as Lilburne and Tarantola (2009) suggested, a crude parameter space is more feasible for exploratory analysis without sufficient prior knowledge, our results showed that a prior constraint on sampling space was sometimes needed when applying SSA. The poorly defined space resulted in the in-stream denitrification being overwhelmingly dominant, which masked the influences of other important processes (Figures 4a and 4b). This is because the inadequate range of *fDeniw* led to an excess effect on NO_3-N concentrations, which largely controlled the model performance. A similar explanation seems to apply when comparing the parameter sensitivity before and after constraining the hydrological parameters: the dominant parameters shifted from the initial steps (soil moisture dynamics: *fKs*, *fPET*) to later steps (infiltration and runoff generation: *fInf*, *fInterf*, *fPerco*) in the process cascade in the hydrological sub-model from PS3 to PS4 (Figures 4c and 4d). This is because in DMC, a headwater catchment where ET accounts for ~80% of annual precipitation, the water storage dynamics and subsequent runoff generation is strongly influenced by ET, especially in a wide parameter space, which leads to the damped sensitivity of other parameters.

Besides the ranking between parameters, inadequate parameter sampling could also bias the spatial patterns of parameter sensitivity. In PS1 and 2, almost all parameters exhibited a higher sensitivity when closer to the outlet (Figures 4a and 4b). Being over-influential, the grids near the evaluation gauge already determined its NO_3-N dynamics, which impeded the transfer of influences from upstream grids. Such proximity to the outlet has been summarized as one of the controlling factors on parameter sensitivity in several SSA studies (e.g., Tang et al., 2007; van Werkhoven et al., 2008; Yang et al., 2019). Though this pattern is unsurprising as grids closer to the evaluation gauge would inevitably exert more influence on simulations, it is important to recognize that as is observed in our catchment, a fully location-dependent pattern probably means the spatial information in sensitivity results is masked by inadequate sampling space, which needs to be adjusted.

This leads to a subsequent question on how to adjust/constrain the parameter space. Here, a LH-sampling-based approach was used by simply iterating the simulation with 10,000 random generations (Figure 3 and Figure S5 in Supporting Information S1). It effectively identified the parameter space for realistic hydrological simulations, but failed to constrain parameters for NO_3-N simulations. This likely reflects the increased potential of equifinality from hydrological to NO_3-N simulations, as the parameter number almost doubled when activating the NO_3-N module (Yang et al., 2019). Such increase in model complexity and risk of equifinality has been

emphasized in other water quality models (Bailey & Ahmadi, 2014; Haas et al., 2015; Wade et al., 2006), as most model development emphasized predictive performance (the ability of a model to accurately reproduce each observed variable) at the cost of functional performance (the ability of a model to correctly simulate individual biogeophysical processes and their interactions) (Ruddell et al., 2019). Moreover, a disconnected relationship between the hydrological and NO_3-N simulations (i.e., the negative correlation between the performance for discharge and in-stream NO_3-N in Figure S4 of Supporting Information S1) was observed, which contrasts with previous findings that NO_3-N dynamics could only be simulated satisfactorily with a reasonable simulation of key runoff components (Hesser et al., 2010). Such disconnection of hydrological and NO_3-N simulations significantly increased the difficulty in identifying the effective sampling space. An alternative solution would be a more target-oriented and efficient algorithm, for example, Bayesian search (Vrugt et al., 2009), to better constrain the sampling space and achieve fully "behavioral" parameter sets (Z. Chen et al., 2017). However, the derived space would need to be carefully checked for both hydrological and NO_3-N performances, regarding the disconnection stated above and the risk of local optima. Similarly, such disconnection also poses the necessity to include both hydrological and NO_3-N states/fluxes into model calibration (in the form of multi-objective error function).

4.2. Parameter Sensitivity and Their Influential Domain

Spatial analysis of parameter sensitivity is a useful tool to guide management practice as its results can be interpreted as being indicative of relative process dominance when the model is assumed to accurately conceptualize catchment behavior and functioning (Wagener & Pianosi, 2019). Therefore, investigating how parameter dominance spatially varies can potentially identify the dominant processes in nature, and provide an evidence base for management (Reusser et al., 2011; Sieber & Uhlenbrook, 2005).

Among the six hydrological parameters, *fSnow* was the only one identified as insensitive in all sampling schemes (Figure 4). This reflects the negligible contribution from snow melt to hydrological fluxes in DMC, which would likely be different in snow-dominated catchments (Berezowski et al., 2015; Reusser et al., 2011). Similarly, the sensitivity of *fMinlr* remained damped although mineralization greatly contributed to the NO_3-N balance in the catchment (25%–30%, S. Wu et al., 2022), which is consistent with another SSA study in central Germany (Yang et al., 2019). This is likely related to the concept and structure of the NO_3-N sub-model, which regards mineralization as a relatively stable process (Lindström et al., 2010; Yang et al., 2019). Instead, mineralization could become influential when plowing was introduced into the simulation (Howden et al., 2011). The *fNpprt* was also insensitive and mainly attributed to the generally low discharge given the high PET and low slopes in DMC. However, uncertainty in *fNpprt* behavior should be recognized, as in water quality modeling, in-stream NO_3-N removal between denitrification (*fDeniw*) and assimilatory (*fNpprt*) uptake can be highly confounded (Wollschläger et al., 2017), which may increase potential equifinality.

The rest of the parameters were sensitive, which includes those controlling most hydrological processes (infiltration, percolation, and runoff generation) and denitrification, given they were influential in at least one sampling space. Though varying between different sampling space, sensitivity of most parameters (*fKs*, *fInf*, *fInterf*, *fPerco*, *fDenis*) followed the arable land distribution (Figure 1b). This is because, like other NO_3-N modeling (Howden et al., 2011; Taylor et al., 2016), the extensive NO_3-N excess from fertilizer and manure applications was the primary driving force of NO_3-N simulations, and was responsible for the increase in both local and downstream concentrations in DMC. Higher parameter sensitivity in NO_3-N rich regions has also been observed in a previous SSA study (Yang et al., 2019), and the importance of conceptualizing NO_3-N supply was confirmed in Saint-Geours and Lilburne et al. (2010) by directly incorporating land use information as an input of SSA.

Another factor that potentially controlled the spatial sensitivity was the hydrological transport capacity, as higher sensitivity generally occurred in areas with higher hydrological fluxes. However, it is difficult to disentangle such impacts from the NO_3-N supply, as distribution of hydrological fluxes also followed the land use, exhibiting higher infiltration, percolation and runoff generation in arable land (where N inputs are highest) compared to forested areas (Figure 1d). This pattern was based on the nearly homogenous distribution of precipitation and soil properties (sand and clay proportion) in DMC, which led to the hydrological fluxes being dominated by the vegetation cover (higher ET loss in forest than crop/grassland in agricultural land; Smith et al., 2021). In other catchments with strong heterogeneity in precipitation (Tang et al., 2007; van Werkhoven et al., 2008; Wagener et al., 2009) or soil properties (Yang et al., 2019), the hydrological transport capacity could be the dominant factor for parameter sensitivity regardless of land cover.

4.3. Longer-Term Shifts in Dominant Processes

While the dominant parameters in key "hot spots" and influential areas was derived from the spatial characteristics of parameter sensitivity, time-varying SSA helped to identify the critical periods over the past 30 years where controls on water quality differed. The long-term distributed data in DMC thus leveraged novel insights for SSA application in water quality models. Generally, though varying in absolute values, the sensitivity indices consistently showed similar temporal trends with both performance metrics (RMSE in Figure 5; Pbias in Figure S8 of Supporting Information S1), being higher in wetter years. This suggested that the bias in NO_3-N simulation over a long-term period more likely originated from wet periods, which is expected as NO_3-N transport aligns with hydrological fluxes, and NO_3-N transformations largely rely on soil moisture conditions either in the mHM-Nitrate formulation (Yang et al., 2019) or real world (Seitzinger et al., 2006). Such changes resulted in accumulation and mobilization patterns of terrestrial NO_3-N in dry and wet periods, respectively, and thus higher concentrations and variability in wetter years in DMC (S. Wu et al., 2021), which was consistent with many other lowland catchments (e.g., Dupas et al., 2016; Outram et al., 2016).

Another interesting finding is the increase in sensitivity of in-stream and soil denitrification (*fDeniw* and *fDenis*) after land management changes (Figure 5). This is consistent with local knowledge in DMC, as both cessation of drainages and wetland restoration increased the water residence time in soils and channel networks, and enhanced NO_3-N loss through denitrification (Hansen et al., 2018; Smith et al., 2020). Such shift in sensitivity highlights how NO_3-N transformations can be fundamentally affected by management changes despite hydroclimatic inputs being consistent, which further underlines the necessity to incorporate more detailed descriptions of land management into models, or directly recalibrating for periods after major management change (Rode et al., 2009; Taylor et al., 2016).

Though wet years were identified as critical periods from the absolute values of sensitivity, the extracted information was limited as generally all parameters followed the same temporal trend. Therefore, the relative sensitivity was calculated in each timestep, as presented in Section 2.5, to explore which parameter was dominant over the long-term period and how the dominance changed (Figure 6). From a hydrological perspective, shifts in dominance of hydrological processes were observed from dry to wet periods (Figures 6, 7, and Figure S16 in Supporting Information S1), that is, from the parameters in the upper soil column (*fPET* and *fInf*) to the lower soil columns and underlying aquifer (*fInterf* and *fPerco*). The dominant influence of ET-related parameters under low-flow conditions has been reported in previous time-varying SA studies (Guse et al., 2014, 2016; Pfannerstill et al., 2015; Y. Wu & Liu, 2012). Such patterns can potentially be attributed to the dominant role of ET in DMC (accounting for >80% of annual precipitation; see Smith et al., 2021), which resulted in water availability and hydrological transport largely depending on canopy and soil ET. This effect is then extended for *fInf*, as infiltration is also the dominant process within soil columns in mHM-Nitrate and dependent on net rainfall. In the other words, water distribution in dry years was determined by the processes in soil (upper) layers, resulting in limited lateral flow generation at grid scale and thus damped hydrological connectivity at the catchment scale. In wet years however, the dominance gradually shifted to dynamics of the gravitational water drainage given the increased relative sensitivity of *fInterf* and *fPerco* (Figures 6 and 7). Similar increased sensitivity in deeper layers and aquifers with greater annual precipitation was also reported in Basijokaite and Kelleher (2021). Such a shift in dominance emphasizes that monitoring and modeling should be cognizant of changing wetness conditions, and highlights the generic importance of long-term datasets in water quality models.

In terms of NO_3-N parameters, temporal dynamics could be grouped by locations of influence; as terrestrial (*fDenis* and *fMinlr*) and in-stream parameters (*fDeniw* and *fNpprt*) dominated the wet and dry periods, respectively (Figure 7). This is conceptually unsurprising as both rates of soil denitrification and mineralization are intrinsically related to moisture conditions (Seitzinger et al., 2006). Additionally, higher hydrological fluxes in wet years could better transfer their influence (within soil columns) to deeper layers and underlying aquifers as well as downstream. In contrast, in-stream processes were more dominant in dry years, which confirms observations in other catchments where the relative importance of in-stream biogeochemical reactions was enhanced under low flow periods (Bechtold et al., 2003; Moatar et al., 2017) due to the increase in water residence time in the channel network (Smith et al., 2021). Such gradual shift in dominance emphasized that both terrestrial and in-stream denitrification need to be included in future monitoring schemes; especially in-stream processes, considering the recent prolonged droughts (Kleine et al., 2020) and projected increases in drought frequency in coming decades (Nikulin et al., 2011).

4.4. Wider Implications and Future Work

Though the influential parameters, and their spatial domains and time periods were successfully identified in DMC, there are still two core questions to further address: how can these results (from time-varying SSA) contribute to the community of water quality modelers, and how to transfer such knowledge to other catchments or models?

Like the many SAs applied for dynamic earth system models which are indicative of relative parameter importance, regardless of what the optimal parameter set may be (Gupta & Razavi, 2018; Razavi et al., 2021), the SSA in this study shares the same goal of identifying the parameters that most strongly affect the magnitude, variability, and dynamics of model response (Razavi & Gupta, 2015). The main difference is that by disentangling the parameterization at spatial (grid-wise) and temporal (1-year moving window) scales, SSA not only identified *which* parameter(s) was(were) influential, but *where* and *when* these influences occurred. Such "*WWW*" information has a strong potential to: (a) evaluate the current model structure, (b) guide future model development, and (c) the evolution of observation networks.

When high sensitivity indices μ^* of a parameter are found over a specific catchment area, it means the underlying parameter together with the corresponding process exerts a strong influence on the outlet simulation. In contrast, in the rest insensitive domain, the parameter is inactive and no information is available for adjusting the parameter to a better value (Wagener et al., 2009). Therefore, the spatial pattern of parameter sensitivity is informative in terms of evaluating the parameterization scheme, as it means one parameter could be spatially aggregated within its inactive domain, but needs to be explicitly considered in its active domain. In this particular application to DMC, all terrestrial NO_3-N parameters shared the same active domain, that is, arable land in the upper catchment. This spatial pattern in general agreed with the current parameterization scheme in mHM-Nitrate which assigned NO_3-N parameters based on land-use types (see the SA results under original parameterization scheme in Figure S17 of Supporting Information S1). Such a pattern suggested that in this study case, NO_3-N parameterization could be further disentangled into finer land use categories (e.g., pasture, or croplands with different rotation strategies) in agricultural-related regions, while in non-agricultural regions (i.e., three different forest types), the parameters could be aggregated to balance the increased computational demands. This knowledge, that is, parametrizing the NO_3-N parameters explicitly for arable land, should be transferable to other agricultural catchments given the dominant role of anthropogenic inputs (Howden et al., 2011; Taylor et al., 2016). However, it is important to check the temporal dynamics of parameter sensitivity, as some apparently insensitive parameters can still be influential during specific periods, as previously reported (Herman et al., 2013a) and demonstrated in this study (e.g., *fSnow* in colder, wetter years). As for the10 hydrological parameters, the contradictions between the parameterization strategy (spatially constant) and the spatial pattern of sensitivity (land use-dependent) suggested potential benefits from resolving the parameterization into a finer level. However, it is difficult to judge conclusively given that these parameters were conceptualized intrinsically as "global parameters" in mHM (Samaniego et al., 2010). Moreover, the disconnection between the performance of hydrological and NO_3-N simulations (Section 4.1) makes the suggestion less convincing as we used outlet NO_3-N as the evaluation target for SSA, while different conclusions could be drawn if SSA was conducted against outlet discharge or other hydrological states/fluxes (e.g., soil moisture or groundwater level). However, it is possible to transfer the method itself to other hydrological models, if SSA is conducted against hydrological fluxes of interest.

Besides evaluating the model parameterization, SSA results are also generically informative in guiding prioritization in model development. This is because disentangling both spatial and temporal aspects of sensitivity offers an opportunity to examine the correlations between spatiotemporal sensitivity patterns, and the catchment characteristics or hydrological/NO_3-N fluxes. This can demonstrate not only *which* parameter(s) was(were) influential, but also potentially *why*. In DMC for example, a key insight was that the temporal pattern of sensitivity indices μ^* of *fDenis* was positively correlated with annual wetness conditions but negatively with the NO_3-N concentration in top soils. This shows that the soil denitrification was depressed in dry years as the NO_3-N was immobilized in the top soil due to limited vertical transport capacity. Therefore, an obvious important process-based goal for further model refinement would be to improve the representation of NO_3-N transport in the soil by measuring and modeling the depth-dependent profiles of NO_3-N concentrations in soil water under different wetness conditions, and incorporating this as an empirical module in mHM-Nitrate. Although like most model diagnostic techniques, SSA provides no specific guidance on how to reprogram the model (Ruddell et al., 2019), it takes a step forward

on identifying *where* to refine by attributing the model sensitivity to specific processes via checking the correlation with key states and fluxes (rather than a set of influential parameters in traditional SA).

To authors knowledge, our study is one of the first time-varying SSA applications in the field of NO_3-N modeling. This analysis, with the advantages noted, has potential transferability to other catchments and models, since all the basic concepts in SSA are adopted from the Morris method (Campolongo et al., 2007) without any new assumption. However, one should recognize the uncertainty in SA, since insights into catchment functioning are only possible if it is conducted based on adequate information and methodological setting (Gupta & Razavi, 2018). In terms of SSA, similarly, different settings can result in contrasting conclusions (Baroni et al., 2017); for example, the parameters characterizing deep aquifers have been reported to be more influential in low-flow conditions for discharge simulation (Guse et al., 2016; Massmann & Holzmann, 2012; Pfannerstill et al., 2015), while Basijokaite and Kelleher (2021) and our study found increased sensitivity during wet periods instead. Here we take DMC as an exemplar to briefly introduce how these key factors/methodological settings altered the results during SSA implementation.

The first factor is the parameter selection for SSA. In most previous studies, only a few key components were included in the analysis, while in this study a more complete sequence of 10 hydrological and NO_3-N processes was explored. For example, while ET-related parameters are often excluded from SSA (Herman et al., 2013a; Reusser et al., 2011), they proved to be influential in this study due to the ET-dominance in the study catchment. Consequently, the relative sensitivity of parameters in deeper layers and the underlying aquifer were inevitably contingent on the dominance of *fPET*, given that interflow and groundwater flow only accounted for 10% and 8% of annual precipitation respectively (S. Wu et al., 2022). The second reason is the window length. While most studies selected a sub-annual window from hours (Z. Chen et al., 2017), days (Haas et al., 2015; Herman et al., 2013b; Pfannerstill et al., 2015), weeks (Bailey & Ahmadi, 2014; Guse et al., 2014) to months (L. Chen et al., 2019; Guse et al., 2016), a 1-year moving window was used in this study. The window length can alter the sensitivity ranking between parameters and regulate their temporal dynamics (L. Chen et al., 2019; Massmann & Holzmann, 2012), and in our case, conducting SA at annual scale means the loss of details at sub-annual scale. However, this is related to our weekly based NO_3-N observations. Another factor was the evaluation metric. In this study, parameter sensitivity was assessed only based on an integrative measurement (i.e., in-stream NO_3-N concentration) at the catchment outlet. Therefore, internal model behavior could somewhat remain untackled, which could be improved in future studies with multi-objective functions. The final reason was the selection of SA method. While many studies employed Sobol' (Z. Chen et al., 2017) or FAST methods (Haas et al., 2015; Pfannerstill et al., 2015), the Morris method (Campolongo et al., 2007) was used here. Although its capacity to benchmark against the Sobol' variance decomposition has been demonstrated with significantly reduced iterations (Herman et al., 2013b), the disadvantage of the Morris method is that it cannot estimate individual interactions between parameters, whereas giving only the overall interaction of a parameter with the rest of the model (Shin et al., 2013). Such uncertainty could lead to the non-identifiability of some sensitive parameters given their strong interactions (with other parameters), though expected to be more damped in annual compared to seasonal or event scale applications (Massmann & Holzmann, 2012). For our application, nearly two weeks of run times were required with parallel use of 20 CPUs, which means the analysis would be intractable using Sobol or FAST method, as at least three more times of iterations would be required for sensitivity convergence (Herman et al., 2013b).

A potential solution to the expensive computation demand is reducing the spatial resolution. In this study, the model domain was disaggregated into 185 grids, which exceeded the settings in most previous studies, for example, 31 in Tang et al. (2007), 78 in van Werkhoven et al. (2008), and 78 grids in Herman et al. (2013a). A coarse resolution can substantially reduce the computational demand given the required iterations of SSA is determined by the number of grid cells and parameters. Moreover, in authors' opinion, a finer resolution in SSA doesn't always equal an improved spatial representation, because the potential for compensating effects over the spatial domain increase (Beven & Freer, 2001). During the analysis of the SSA results, we found that the variability of simulated in-stream NO_3-N significantly decreased along the stream (Figure S18 in Supporting Information S1). This is because the simulation in a local grid represents the integration of results from all upstream grids, and thus it is more likely that the influences from these stochastically sampled parameters in upstream grids compensate each other, when resolution is higher and more grids are involved. In the other words, a finer resolution for SSA would lead to a stronger constraint on the ranges of simulated results; and theoretically, in-stream NO_3-N at

the outlet would be near-constant if the resolution is extremely high. These compensating errors are, of course, negligible when simply applying a model, because the model domain is generally spatially aggregated (based on land use, soil types, etc.). However, it needs to be considered in any diagnostic analysis that introduces stochastic factors in a spatially explicit way (grid-wise, see Herman et al. [2013a] and Yang et al. [2019]). To authors knowledge, such compensating effects have seldom been clarified in previous SSA, as most studies focused more on the extent and representativeness of the sampling space, rather than the range of simulation results. This emphasizes the importance of spatial resolution as an additional crucial factor in time-varying SSA, which should seek to achieve a balance between spatial details, computation demands, and compensating effects depending on the research aim.

5. Conclusions

Distributed models have been increasingly applied in hydrological and water quality studies, providing greater spatiotemporal resolution, but increasing uncertainty and the risk of equifinality. Therefore, an approach for time-varying spatial sensitivity analysis was presented in this study, aiming to identify the most important parameters, areas within the model domain, and time periods for NO_3-N simulation in a grid-based nitrate model (mHM-Nitrate). To achieve this goal, the Morris method was employed for computing the sensitivity of key hydrological and NO_3-N parameters in each grid against 30-year NO_3-N observation, either for the whole period or using a 1-year moving window, with four different methods for parameter space sampling.

Results showed the parameter sensitivity differed within sampling spaces, and an overly wide range for a specific parameter (i.e., aquatic denitrification rates) could bias the sensitivity of the remaining parameters, leading to their spatial pattern only related to the proximity to outlet. Therefore, a constraint based on model performance on parameter space is necessary for SSA.

Among all the sampling spaces, parameters related to soil moisture balance (*fKs*), evapotranspiration (*fPET*), and aquatic (*fDeniw*) and soil denitrification (*fDenis*) were most influential, while parameters in infiltration (*fInf*), interflow (*fInterf*) and groundwater flow (*fPerco*) modules also showed moderate impacts on NO_3-N simulation. The remaining parameters, including snow (*fSnow*), aquatic assimilation (*fNpprt*), and soil mineralization (*fMinlr*) were identified as insensitive. Spatial sensitivity of most parameters followed the land use distribution, exerting more influence on NO_3-N simulation in areas with higher NO_3-N supply and hydrological transport capacity.

In-terms of temporal dynamics, all the parameters showed higher sensitivity in wetter years. A moderate increase in sensitivity of denitrification parameters was also found after wetland restoration, suggesting the necessity to consider land management change in modeling application. To better unravel the dominant processes, the relative proportion of sensitivity was calculated via dividing the sensitivity of a parameter by the cumulative sensitivity of all parameters. The results showed a shift in the dominance of hydrological parameters in relation to hydroclimate: parameters related to ET and infiltration in the soil profile dominated dry periods, while those regulating runoff processes in deeper layers and underlying aquifers exerted more influence in wet periods. As for NO_3-N parameters, the in-stream and terrestrial processes were, respectively, dominant in dry and wet years. Such temporal pattern highlighted that the focus on different processes should be adapted based on wet or dry conditions, either for model calibration or monitoring scheme.

Finally, the SSA results were used to evaluate the model structure as it identifies not only *which* parameter(s) is(are) influential, but *where* and *when* such influences occur. The current NO_3-N parameterization scheme was supported since the spatial pattern of parameter sensitivity aligned with the parameterization (land use-dependent), while contradictions between the hydrological parameterization strategy (spatially constant) and spatial sensitivity pattern (land use-dependent) suggest a potential improvement of hydrological parameterization (downscaling from global to land use-dependent). However, uncertainty could arise from different methodological settings during SSA implementation, including the selection of parameters, their bounds, window length, analysis method, and spatial resolution.

Appendix A

The appendix contains Table A1 introducing the abbrevations in the main text.

Table A1
Abbreviations in Figure 7 and Figure S2 in Supporting Information S1

Abbreviations	Unit	Description
SumHy	-	The cumulative relative sensitivity of all hydrological parameters
Pre	mm	Precipitation
SoilMoist1-3	mm	Soil moisture in soil layer 1–3
AET	mm	Actual evapotranspiration
InfilSoil1-3	mm	Infiltration from soil layer 1–3
Perco	mm	Percolation from soil layer 3 to deeper aquifer
SlowRunoff	mm	Interflow generation
Baseflow	mm	Groundwater flow generation
TotalRunoff	mm	Cumulative runoff generation (interflow + groundwater flow)
cSoilMoist1-3	mg/L	NO_3-N concentrations in soil layer 1–3
cSlowRunoff	mg/L	NO_3-N concentrations in interflow
cBaseflow	mg/L	NO_3-N concentrations in groundwater flow
cTotalRunoff	mg/L	NO_3-N concentrations in cumulative runoff
cDischarge	mg/L	NO_3-N concentrations in discharge
SoilUptake	kg/ha	Soil nitrogen uptake by plants
SoilMinlr	kg/ha	Soil mineralization
SoilDeni	kg/ha	Soil denitrification
AquaticDeni	kg/ha	In-stream denitrification

Data Availability Statement

For the source codes of time-varying spatial sensitivity analysis and geographic datasets please refer to https://doi.org/10.5281/zenodo.6497225. The NO_3-N time series is available in https://fred.igb-berlin.de/data/package/629.

Acknowledgments
Songjun Wu is funded by the Chinese Scholarship Council (CSC). Contributions from Chris Soulsby are supported by the Leverhulme Trust through the ISO-LAND project (Grant Nos. RPG 2018 375). Tetzlaff's contribution was partly funded through the Einstein Research Unit "Climate and Water under Change" from the Einstein Foundation Berlin and Berlin University Alliance. We thank the German Weather Service (DWD) for providing meteorological data set. The staff of the IGB chemical analytics and biogeochemistry lab are thanked for compiling the long-term water quality data set in DMC. Open Access funding enabled and organized by Projekt DEAL.

References

Anderton, S., Latron, J., & Gallart, F. (2002). Sensitivity analysis and multi-response, multi-criteria evaluation of a physically based distributed model. *Hydrological Processes*, *16*(2), 333–353. https://doi.org/10.1002/hyp.336

Bahremand, A., & De Smedt, F. (2008). Distributed hydrological modeling and sensitivity analysis in Torysa Watershed, Slovakia. *Water Resources Management*, *22*(3), 393–408. https://doi.org/10.1007/s11269-007-9168-x

Bailey, R. T., & Ahmadi, M. (2014). Spatial and temporal variability of in-stream water quality parameter influence on dissolved oxygen and nitrate within a regional stream network. *Ecological Modelling*, *277*, 87–96. https://doi.org/10.1016/j.ecolmodel.2014.01.015

Baroni, G., Zink, M., Kumar, R., Samaniego, L., & Attinger, S. (2017). Effects of uncertainty in soil properties on simulated hydrological states and fluxes at different spatio-temporal scales. *Hydrology and Earth System Sciences*, *21*(5), 2301–2320. https://doi.org/10.5194/HESS-21-2301-2017

Basijokaite, R., & Kelleher, C. (2021). Time-varying sensitivity analysis reveals relationships between watershed climate and variations in annual parameter importance in regions with strong interannual variability. *Water Resources Research*, *57*(1), e2020WR028544. https://doi.org/10.1029/2020WR028544

Bechtold, J. S., Edwards, R. T., & Naiman, R. J. (2003). Biotic versus hydrologic control over seasonal nitrate leaching in a floodplain forest. *Biogeochemistry*, *63*(1), 53–72. https://doi.org/10.1023/A:1023350127042

Berezowski, T., Nossent, J., Chormański, J., & Batelaan, O. (2015). Spatial sensitivity analysis of snow cover data in a distributed rainfall-runoff model. *Hydrology and Earth System Sciences*, *19*(4), 1887–1904. https://doi.org/10.5194/hess-19-1887-2015

Bergström, S. (1995). The HBV model. *Computer models of watershed hydrology* (pp. 443–476).

Beven, K., & Freer, J. (2001). Equifinality, data assimilation, and uncertainty estimation in mechanistic modeling of complex environmental systems using the GLUE methodology. *Journal of Hydrology*, *249*(1–4), 11–29. https://doi.org/10.1016/S0022-1694(01)00421-8

Bösel, B. (2018). Personal interview.

Bouraoui, F., & Grizzetti, B. (2011). Long term change of nutrient concentrations of rivers discharging in European seas. *Science of the Total Environment*, *409*(23), 4899–4916. https://doi.org/10.1016/J.SCITOTENV.2011.08.015

Campolongo, F., Cariboni, J., & Saltelli, A. (2007). An effective screening design for sensitivity analysis of large models. *Environmental Modelling & Software*, *22*(10), 1509–1518. https://doi.org/10.1016/J.ENVSOFT.2006.10.004

Chen, L., Chen, S., Li, S., & Shen, Z. (2019). Temporal and spatial scaling effects of parameter sensitivity in relation to non-point source pollution simulation. *Journal of Hydrology*, *571*, 36–49. https://doi.org/10.1016/j.jhydrol.2019.01.045

Chen, Z., Hartmann, A., & Goldscheider, N. (2017). A new approach to evaluate spatiotemporal dynamics of controlling parameters in distributed environmental models. *Environmental Modelling & Software*, *87*, 1–16. https://doi.org/10.1016/j.envsoft.2016.10.005

Clark, M. P., Bierkens, M. F., Samaniego, L., Woods, R. A., Uijlenhoet, R., Bennett, K. E., et al. (2017). The evolution of process-based hydrologic models: Historical challenges and the collective quest for physical realism. *Hydrology and Earth System Sciences*, *21*(7), 3427–3440. https://doi.org/10.5194/hess-21-3427-2017

Cornelissen, T., Diekkrüger, B., & Bogena, H. R. (2016). Using high-resolution data to test parameter sensitivity of the distributed hydrological model HydroGeoSphere. *Water*, *8*(5), 202. https://doi.org/10.3390/w8050202

Crosetto, M., Tarantola, S., & Saltelli, A. (2000). Sensitivity and uncertainty analysis in spatial modelling based on GIS. *Agriculture, Ecosystems & Environment*, *81*(1), 71–79. https://doi.org/10.1016/S0167-8809(00)00169-9

Demirel, M. C., Koch, J., Mendiguren, G., & Stisen, S. (2018). Spatial pattern oriented multicriteria sensitivity analysis of a distributed hydrologic model. *Water*, *10*(9), 1188. https://doi.org/10.3390/w10091188

Dickinson, R. E. (1984). Modeling evapotranspiration for three-dimensional global climate models. *Climate Processes and Climate Sensitivity*, *29*, 58–72. https://doi.org/10.1029/GM029p0058

Dupas, R., Jomaa, S., Musolff, A., Borchardt, D., & Rode, M. (2016). Disentangling the influence of hydroclimatic patterns and agricultural management on river nitrate dynamics from sub-hourly to decadal time scales. *Science of the Total Environment*, *571*, 791–800. https://doi.org/10.1016/j.scitotenv.2016.07.053

EMEP. (2001). *The co-operative programme for the monitoring and evaluation of the long-range transmission of air pollutants in Europe*. EMEP Measurement Database. Retrieved from http://www.emep.int/

Galloway, J. N., Townsend, A. R., Erisman, J. W., Bekunda, M., Cai, Z., Freney, J. R., et al. (2008). Transformation of the nitrogen cycle: Recent trends, questions, and potential solutions. *Science*, *320*(5878), 889–892. https://doi.org/10.1126/science.1136674

Ghasemizade, M., Baroni, G., Abbaspour, K., & Schirmer, M. (2017). Combined analysis of time-varying sensitivity and identifiability indices to diagnose the response of a complex environmental model. *Environmental Modelling & Software*, *88*, 22–34. https://doi.org/10.1016/j.envsoft.2016.10.011

Gill, M. A. (1978). Flood routing by the Muskingum method. *Journal of Hydrology*, *36*(3–4), 353–363. https://doi.org/10.1016/0022-1694(78)90153-1

Green, P. A., Vörösmarty, C. J., Meybeck, M., Galloway, J. N., Peterson, B. J., & Boyer, E. W. (2004). Pre-industrial and contemporary fluxes of nitrogen through rivers: A global assessment based on typology. *Biogeochemistry*, *68*(1), 71–105. https://doi.org/10.1023/B:BIOG.0000025742.82155.92

Grizzetti, B., Passy, P., Billen, G., Bouraoui, F., Garnier, J., & Lassaletta, L. (2015). The role of water nitrogen retention in integrated nutrient management: Assessment in a large basin using different modelling approaches. *Environmental Research Letters*, *10*(6), 065008. https://doi.org/10.1088/1748-9326/10/6/065008

Gupta, H. V., & Razavi, S. (2018). Revisiting the basis of sensitivity analysis for dynamical Earth system models. *Water Resources Research*, *54*(11), 8692–8717. https://doi.org/10.1029/2018WR022668

Guse, B., Pfannerstill, M., Strauch, M., Reusser, D. E., Lüdtke, S., Volk, M., et al. (2016). On characterizing the temporal dominance patterns of model parameters and processes. *Hydrological Processes*, *30*(13), 2255–2270. https://doi.org/10.1002/hyp.10764

Guse, B., Reusser, D. E., & Fohrer, N. (2014). How to improve the representation of hydrological processes in SWAT for a lowland catchment–temporal analysis of parameter sensitivity and model performance. *Hydrological Processes*, *28*(4), 2651–2670. https://doi.org/10.1002/hyp.9777

Haas, M. B., Guse, B., Pfannerstill, M., & Fohrer, N. (2015). Detection of dominant nitrate processes in ecohydrological modeling with temporal parameter sensitivity analysis. *Ecological Modelling*, *314*, 62–72. https://doi.org/10.1016/j.ecolmodel.2015.07.009

Hall, J., Tarantola, S., Bates, P., & Horritt, M. (2005). Distributed sensitivity analysis of flood inundation model calibration. *Journal of Hydraulic Engineering*, *131*(2), 117–126. https://doi.org/10.1061/(ASCE)0733-9429(2005)131:2(117)

Hansen, A. T., Dolph, C. L., Foufoula-Georgiou, E., & Finlay, J. C. (2018). Contribution of wetlands to nitrate removal at the watershed scale. *Nature Geoscience*, *11*(2), 127–132. https://doi.org/10.1038/s41561-017-0056-6

Helton, J. C., & Davis, F. J. (2003). Latin hypercube sampling and the propagation of uncertainty in analyses of complex systems. *Reliability Engineering & System Safety*, *81*(1), 23–69. https://doi.org/10.1016/S0951-8320(03)00058-9

Herman, J., Kollat, J., Reed, P., & Wagener, T. (2013a). From maps to movies: High-resolution time-varying sensitivity analysis for spatially distributed watershed models. *Hydrology and Earth System Sciences*, *17*(12), 5109–5125. https://doi.org/10.5194/hess-17-5109-2013

Herman, J., Kollat, J., Reed, P., & Wagener, T. (2013b). Method of Morris effectively reduces the computational demands of global sensitivity analysis for distributed watershed models. *Hydrology and Earth System Sciences*, *17*(7), 2893–2903. https://doi.org/10.5194/hess-17-2893-2013

Herman, J., Reed, P., & Wagener, T. (2013). Time-varying sensitivity analysis clarifies the effects of watershed model formulation on model behavior. *Water Resources Research*, *49*(3), 1400–1414. https://doi.org/10.1002/wrcr.20124

Hesser, F. B., Franko, U., & Rode, M. (2010). Spatially distributed lateral nitrate transport at the catchment scale. *Journal of Environmental Quality*, *39*(1), 193–203. https://doi.org/10.2134/JEQ2009.0031

Hostache, R., Lai, X., Monnier, J., & Puech, C. (2010). Assimilation of spatially distributed water levels into a shallow-water flood model. Part II: Use of a remote sensing image of Mosel River. *Journal of Hydrology*, *390*(3–4), 257–268. https://doi.org/10.1016/j.jhydrol.2010.07.003

Howden, N., Burt, T., Mathias, S., Worrall, F., & Whelan, M. (2011). Modelling long-term diffuse nitrate pollution at the catchment-scale: Data, parameter and epistemic uncertainty. *Journal of Hydrology*, *403*(3–4), 337–351. https://doi.org/10.1016/j.jhydrol.2011.04.012

Hundecha, Y., & Bárdossy, A. (2004). Modeling of the effect of land use changes on the runoff generation of a river basin through parameter regionalization of a watershed model. *Journal of Hydrology*, *292*(1–4), 281–295. https://doi.org/10.1016/j.jhydrol.2004.01.002

Kleine, L., Tetzlaff, D., Smith, A., Wang, H., & Soulsby, C. (2020). Using water stable isotopes to understand evaporation, moisture stress, and re-wetting in catchment forest and grassland soils of the summer drought of 2018. *Hydrology and Earth System Sciences*, *24*(7), 3737–3752. https://doi.org/10.5194/hess-24-3737-2020

Koch, J., Mendiguren, G., Mariethoz, G., & Stisen, S. (2017). Spatial sensitivity analysis of simulated land surface patterns in a catchment model using a set of innovative spatial performance metrics. *Journal of Hydrometeorology*, *18*(4), 1121–1142. https://doi.org/10.1175/JHM-D-16-0148.1

Leip, A., Britz, W., Weiss, F., & de Vries, W. (2011). Farm, land, and soil nitrogen budgets for agriculture in Europe calculated with CAPRI. *Environmental Pollution*, *159*(11), 3243–3253. https://doi.org/10.1016/j.envpol.2011.01.040

Lilburne, L., & Tarantola, S. (2009). Sensitivity analysis of spatial models. *International Journal of Geographical Information Science*, *23*(2), 151–168. https://doi.org/10.1080/13658810802094995

Lindström, G., Pers, C., Rosberg, J., Strömqvist, J., & Arheimer, B. (2010). Development and testing of the HYPE (Hydrological Predictions for the Environment) water quality model for different spatial scales. *Hydrology Research*, *41*(3–4), 295–319. https://doi.org/10.2166/nh.2010.007

Massmann, C., & Holzmann, H. (2012). Analysis of the behavior of a rainfall–runoff model using three global sensitivity analysis methods evaluated at different temporal scales. *Journal of Hydrology*, *475*, 97–110. https://doi.org/10.1016/j.jhydrol.2012.09.026

McCuen, R. H. (1973). The role of sensitivity analysis in hydrologic modeling. *Journal of Hydrology*, *18*(1), 37–53. https://doi.org/10.1016/0022-1694(73)90024-3

Meybeck, M. (1982). Carbon, nitrogen, and phosphorus transport by world rivers. *American Journal of Science*, *282*(4), 401–450. https://doi.org/10.2475/ajs.282.4.401

Moatar, F., Abbott, B. W., Minaudo, C., Curie, F., & Pinay, G. (2017). Elemental properties, hydrology, and biology interact to shape concentration-discharge curves for carbon, nutrients, sediment, and major ions. *Water Resources Research*, *53*(2), 1270–1287. https://doi.org/10.1002/2016WR019635

Moreau, P., Viaud, V., Parnaudeau, V., Salmon-Monviola, J., & Durand, P. (2013). An approach for global sensitivity analysis of a complex environmental model to spatial inputs and parameters: A case study of an agro-hydrological model. *Environmental Modelling & Software*, *47*, 74–87. https://doi.org/10.1016/j.envsoft.2013.04.006

Morris, M. D. (1991). Factorial sampling plans for preliminary computational experiments. *Technometrics*, *33*(2), 161–174. https://doi.org/10.1080/00401706.1991.10484804

Musolff, A., Schmidt, C., Selle, B., & Fleckenstein, J. H. (2015). Catchment controls on solute export. *Advances in Water Resources*, *86*, 133–146. https://doi.org/10.1016/j.advwatres.2015.09.026

Nikulin, G., Kjellström, E., Hansson, U., Strandberg, G., & Ullerstig, A. (2011). Evaluation and future projections of temperature, precipitation and wind extremes over Europe in an ensemble of regional climate simulations. *Tellus A: Dynamic Meteorology and Oceanography*, *63*(1), 41–55. https://doi.org/10.1111/j.1600-0870.2010.00466.x

Outram, F. N., Cooper, R. J., Sünnenberg, G., Hiscock, K. M., & Lovett, A. A. (2016). Antecedent conditions, hydrological connectivity and anthropogenic inputs: Factors affecting nitrate and phosphorus transfers to agricultural headwater streams. *Science of the Total Environment*, *545*, 184–199. https://doi.org/10.1016/j.scitotenv.2015.12.025

Pfannerstill, M., Guse, B., Reusser, D., & Fohrer, N. (2015). Process verification of a hydrological model using a temporal parameter sensitivity analysis. *Hydrology and Earth System Sciences*, *19*(10), 4365–4376. https://doi.org/10.5194/hess-19-4365-2015

Razavi, S., & Gupta, H. V. (2015). What do we mean by sensitivity analysis? The need for comprehensive characterization of "global" sensitivity in Earth and Environmental systems models. *Water Resources Research*, *51*(5), 3070–3092. https://doi.org/10.1002/2014WR016527

Razavi, S., Jakeman, A., Saltelli, A., Prieur, C., Iooss, B., Borgonovo, E., et al. (2021). The future of sensitivity analysis: An essential discipline for systems modeling and policy support. *Environmental Modelling & Software*, *137*, 104954. https://doi.org/10.1016/J.ENVSOFT.2020.104954

Reusser, D. E., Buytaert, W., & Zehe, E. (2011). Temporal dynamics of model parameter sensitivity for computationally expensive models with the Fourier amplitude sensitivity test. *Water Resources Research*, *47*(7). https://doi.org/10.1029/2010WR009947

Rode, M., Thiel, E., Franko, U., Wenk, G., & Hesser, F. (2009). Impact of selected agricultural management options on the reduction of nitrogen loads in three representative meso scale catchments in Central Germany. *Science of the Total Environment*, *407*(11), 3459–3472. https://doi.org/10.1016/j.scitotenv.2009.01.053

Rozemeijer, J., Visser, A., Borren, W., Winegram, M., Velde, Y., Klein, J., & Broers, H. (2016). High-frequency monitoring of water fluxes and nutrient loads to assess the effects of controlled drainage on water storage and nutrient transport. *Hydrology and Earth System Sciences*, *20*(1), 347–358. https://doi.org/10.5194/hess-20-347-2016

Ruddell, B. L., Drewry, D. T., & Nearing, G. S. (2019). Information theory for model diagnostics: Structural error is indicated by trade-off between functional and predictive performance. *Water Resources Research*, *55*(8), 6534–6554. https://doi.org/10.1029/2018WR023692

Saint-Geours, N., & Lilburne, L. (2010). Comparison of three spatial sensitivity analysis techniques (pp. 421–424).

Saltelli, A., Tarantola, S., Campolongo, F., & Ratto, M. (2004). *Sensitivity analysis in practice: A guide to assessing scientific models*. Wiley Online Library.

Samaniego, L., Kumar, R., & Attinger, S. (2010). Multiscale parameter regionalization of a grid-based hydrologic model at the mesoscale. *Water Resources Research*, *46*(5), W05523. https://doi.org/10.1029/2008WR007327

Sarrazin, F., Pianosi, F., & Wagener, T. (2016). Global sensitivity analysis of environmental models: Convergence and validation. *Environmental Modelling & Software*, *79*, 135–152. https://doi.org/10.1016/j.envsoft.2016.02.005

Seitzinger, S., Harrison, J. A., Böhlke, J., Bouwman, A., Lowrance, R., Peterson, B., et al. (2006). Denitrification across landscapes and waterscapes: A synthesis. *Ecological Applications*, *16*(6), 2064–2090. https://doi.org/10.1890/1051-0761(2006)016[2064:dalawa]2.0.co;2

Shin, M. J., Guillaume, J. H. A., Croke, B. F. W., & Jakeman, A. J. (2013). Addressing ten questions about conceptual rainfall-runoff models with global sensitivity analyses in R. *Journal of Hydrology*, *503*, 135–152. https://doi.org/10.1016/J.JHYDROL.2013.08.047

Sieber, A., & Uhlenbrook, S. (2005). Sensitivity analyses of a distributed catchment model to verify the model structure. *Journal of Hydrology*, *310*(1–4), 216–235. https://doi.org/10.1890/1051-0761(2006)016[2064:DALAWA]2.0.CO;2

Smith, A., Tetzlaff, D., Gelbrecht, J., Kleine, L., & Soulsby, C. (2020). Riparian wetland rehabilitation and beaver re-colonization impacts on hydrological processes and water quality in a lowland agricultural catchment. *Science of The Total Environment*, *699*, 134302. https://doi.org/10.1016/j.scitotenv.2019.134302

Smith, A., Tetzlaff, D., Kleine, L., Maneta, M., & Soulsby, C. (2021). Quantifying the effects of land use and model scale on water partitioning and water ages using tracer-aided ecohydrological models. *Hydrology and Earth System Sciences*, *25*(4), 2239–2259. https://doi.org/10.5194/hess-25-2239-2021

Sobol, I. M. (2001). Global sensitivity indices for nonlinear mathematical models and their Monte Carlo estimates. *Mathematics and Computers in Simulation*, *55*(1–3), 271–280. https://doi.org/10.1016/S0378-4754(00)00270-6

Tang, Y., Reed, P., van Werkhoven, K., & Wagener, T. (2007). Advancing the identification and evaluation of distributed rainfall-runoff models using global sensitivity analysis. *Water Resources Research*, *43*(6), W06415. https://doi.org/10.1029/2006WR005813

Taylor, S. D., He, Y., & Hiscock, K. M. (2016). Modelling the impacts of agricultural management practices on river water quality in Eastern England. *Journal of Environmental Management*, *180*, 147–163. https://doi.org/10.1016/j.jenvman.2016.05.002

Tolson, B. A., & Shoemaker, C. A. (2007). Dynamically dimensioned search algorithm for computationally efficient watershed model calibration. *Water Resources Research*, *43*(1), W01413. https://doi.org/10.1029/2005WR004723

Tonkin, M. J., & Doherty, J. (2005). A hybrid regularized inversion methodology for highly parameterized environmental models. *Water Resources Research*, *41*(10), W10412. https://doi.org/10.1029/2005WR003995

van Griensven, A., Meixner, T., Grunwald, S., Bishop, T., Diluzio, M., & Srinivasan, R. (2006). A global sensitivity analysis tool for the parameters of multi-variable catchment models. *Journal of Hydrology*, *324*(1–4), 10–23. https://doi.org/10.1016/j.jhydrol.2005.09.008

van Werkhoven, K., Wagener, T., Reed, P., & Tang, Y. (2008). Rainfall characteristics define the value of streamflow observations for distributed watershed model identification. *Geophysical Research Letters*, *35*(11), L11403. https://doi.org/10.1029/2008GL034162

Vrugt, J. A., Ter Braak, C., Diks, C., Robinson, B. A., Hyman, J. M., & Higdon, D. (2009). Accelerating Markov chain Monte Carlo simulation by differential evolution with self-adaptive randomized subspace sampling. *International Journal of Nonlinear Sciences and Numerical Simulation*, *10*(3), 273–290. https://doi.org/10.1515/IJNSNS.2009.10.3.273

Wade, A. J., Butterfield, D., & Whitehead, P. (2006). Towards an improved understanding of the nitrate dynamics in lowland, permeable river-systems: Applications of INCA-N. *Journal of Hydrology*, *330*(1–2), 185–203. https://doi.org/10.1016/j.jhydrol.2006.04.023

Wagener, T., & Pianosi, F. (2019). What has global sensitivity analysis ever done for us? A systematic review to support scientific advancement and to inform policy-making in Earth system modelling. *Earth-Science Reviews*, *194*, 1–18. https://doi.org/10.1016/j.earscirev.2019.04.006

Wagener, T., van Werkhoven, K., Reed, P., & Tang, Y. (2009). Multiobjective sensitivity analysis to understand the information content in stream-flow observations for distributed watershed modeling. *Water Resources Research*, *45*(2), W02501. https://doi.org/10.1029/2008WR007347

Wellen, C., Kamran-Disfani, A.-R., & Arhonditsis, G. B. (2015). Evaluation of the current state of distributed watershed nutrient water quality modeling. *Environmental Science & Technology*, *49*(6), 3278–3290. https://doi.org/10.1021/es5049557

Wetzel, R. G. (2001). *Limnology: Lake and river ecosystems*. Gulf Professional Publishing.

Wollschläger, U., Attinger, S., Borchardt, D., Brauns, M., Cuntz, M., Dietrich, P., et al. (2017). The Bode hydrological observatory: A platform for integrated, interdisciplinary hydro-ecological research within the TERENO Harz/Central German Lowland Observatory. *Environmental Earth Sciences*, *76*(1), 1–25. https://doi.org/10.1007/s12665-016-6327-5

Wu, S., Tetzlaff, D., Goldhammer, T., & Soulsby, C. (2021). Hydroclimatic variability and riparian wetland restoration control the hydrology and nutrient fluxes in a lowland agricultural catchment. *Journal of Hydrology*, *603*, 126904. https://doi.org/10.1016/J.JHYDROL.2021.126904

Wu, S., Tetzlaff, D., Yang, X., & Soulsby, C. (2022). Disentangling the influence of landscape characteristics, hydroclimatic variability and land management on surface water NO_3-N dynamics: Spatially distributed modelling over 30 years in a lowland mixed land use catchment. *Water Resources Research*, *58*(2), e2021WR030566. https://doi.org/10.1029/2021WR030566

Wu, Y., & Liu, S. (2012). Automating calibration, sensitivity and uncertainty analysis of complex models using the R package Flexible Modeling Environment (FME): SWAT as an example. *Environmental Modelling & Software*, *31*, 99–109. https://doi.org/10.1016/j.envsoft.2011.11.013

Yang, X., Jomaa, S., & Rode, M. (2019). Sensitivity analysis of fully distributed parameterization reveals insights into heterogeneous catchment responses for water quality modeling. *Water Resources Research*, *55*(12), 10935–10953. https://doi.org/10.1029/2019WR025575

Yang, X., Jomaa, S., Zink, M., Fleckenstein, J. H., Borchardt, D., & Rode, M. (2018). A new fully distributed model of nitrate transport and removal at catchment scale. *Water Resources Research*, *54*(8), 5856–5877. https://doi.org/10.1029/2017WR022380